Answer to Reviewer 1

(reviewer comment, author response, change in manuscript)

The authors use a MLR approach applied to the SOCAT CO2 data-base to reconstruct a spatially and temporally resolved data-set from 1998 to 2018 in the European continental shelf. From this data-set the authors analyze the temporal trends of pCO2 during winter in different regions (North Sea, Baltic Sea, Norwegian coast & Barents seas) that are compared to the increase of atmospheric CO2.
A more detailed and in-depth analysis could be made.

For instance, the authors compute the trends based on winter-only data. However, since they have a fully seasonally resolved reconstructed data-set, they could also analyze the temporal trends using summer-only data. Are the trends the same ?
In addition, they could compute the trends using the full annual average, which in principle should provide the most robust estimate of inter-annual variations since it integrates all components of seasonal variations. Are the results for the full annual average the same as the winter-only or the summer-only trends?

We do not use winter-only data for estimating the trends. The trends shown in this manuscript are computed over the entire year. We did compute also winter only and summer only trends for comparison to the other studies. Trends in summer were generally less significant than the all-year or winter-only trends. We agree with Referee#1 that the contribution of the different seasons to the overall trend is an interesting feature that can be investigated further. We therefore added a paragraph addressing the trend in pCO2 for every month.

> The hypothesis, that an earlier or more intense bloom onset is responsible for the relatively low trends in the North Sea is supported by looking at the contributions of the different months to the overall trend. Figure 10 show the trend for each month in the four different regions.

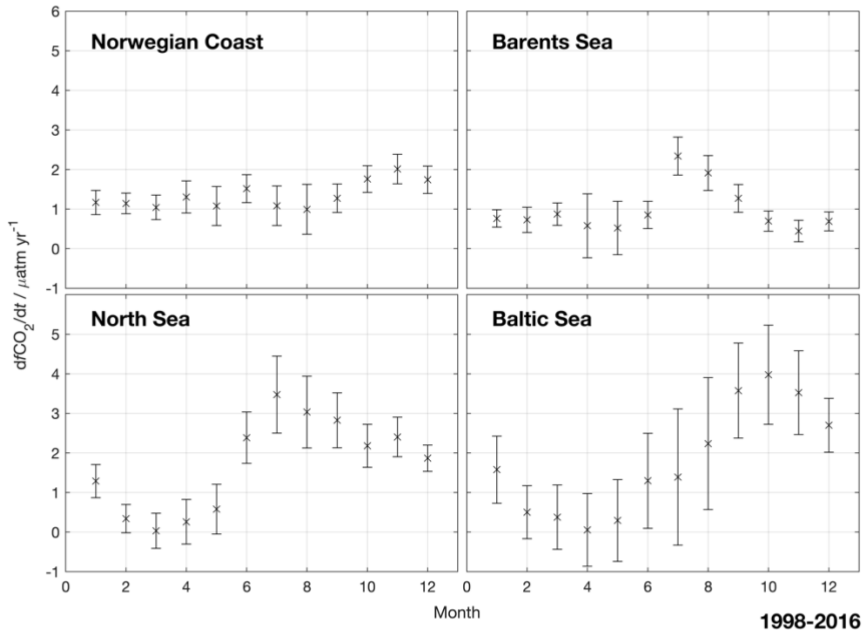

Figure 1 The trend in surface ocean fCO_2 estimated resolved per month (1998 to 2016).

The other question that the authors could attempt to address is how useful is this MRL approach compared the raw SOCAT data-set to compute temporal trends. So, would the analysis of temporal *trends of the raw SOCAT data give the same results as the MRL expanded data-set ? Of course this would require to aggregate the raw data into larger boxes (for instance 3 large boxes for the North Sea: southern bight of the North Sea, Central North Sea and Northern North Sea) to overcome the lower coverage of the raw SOCAT data. This question is motivated by the fact that the European Shelf is one of the areas which is most dense in CO2 data, so that you need to address the question of the usefulness of using a complex MRL approach to reconstruct and gap-fill for an original data-set that is one of the most dense for continental shelves.*

Reviewer 1 is right, when they state, that the European shelfis one of the coastal regions in the world with highest density in CO2 data, especially when looking at the northern North Sea and parts of the Baltic Sea. However, that is not similarly true for all European shelf regions. In the North Sea it would definitely be worthwhile to perform a proper data-based, high resolution trend analysis for the entire basin and then comparing the results to ours. We think, that our manuscript here is not the right place to do so. For the northern part of the North Sea, there is a recent study by (Omar et al., 2019) focusing on winter trends. They find the same trends as we: no significant trend east of about 5E and a trend close to the atmospheric trend west of 5E. We followed also the suggestion of RW1 and performed a quick-and-dirty trend analysis for 9 large boxes (based on deseasonalized gridded SOCAT data from SOCAT v5). The results of this analysis support the results from our maps. We added a table with the SOCAT-based trends to the fCO2 trend section of manuscript and a picture showing the regression analysis to the supplement.
Principally, we do think, that is there is a large value in developing gap filling methods also in regions with a high data density. The major application of gap filled pCO2 products lays not the estimation of trends in pCO2, but in air-sea CO2 fluxes and estimating the ocean carbon sink. For this pCO2 data covering all months, years and regions is crucial.

> The northern European shelf is a region with a high data density. In order to validate the general patterns of $f\mathrm{CO_2}$ trends we estimated the $f\mathrm{CO_2}$ trends also from the SOCAT v5 observations, that was used to produce the MLR (Table 6). We gridded and deseasonalized the SOCAT v5 data and divided the entire region into 9 subregions. A figure showing the fits and the data coverage can be found in Appendix A.
> These directly observation based trends show similar general patterns as those based on our maps (Figure 8, 1998-2016): (1) largest trends in the southern North Sea, (2) decreasing towards the North with trends around the atmospheric trend in the northern North Sea and trends around 1 μatm yr^{-1} in the Barents Sea, (3) close to atmospheric trends in the Baltic Sea.

Region	Latitude / °N	Trend / μatm yr^{-1}
North Sea, South	51 - 54.5	3.2 ± 1.3
North Sea, Center	54.5 - 58	1.43 ± 0.21
North Sea, North	58 - 62	2.320 ± 0.089
Norwegian Coast, South	62 - 68	2.12 ± 0.19
Norwegian Coast, North	68 - 73	1.426 ± 0.099
Barents Sea, South	69 - 74	1.31 ± 0.30
Barents Sea, North	74 - 85	1.01 ± 0.22
Baltic Sea, South	54 - 56	2.05 ± 0.12
Baltic Sea, North	56 - 61	1.84 ± 0.21

Table 1 fCO_2 trend calculated from gridded, deseasonalized SOCAT v5 observations.

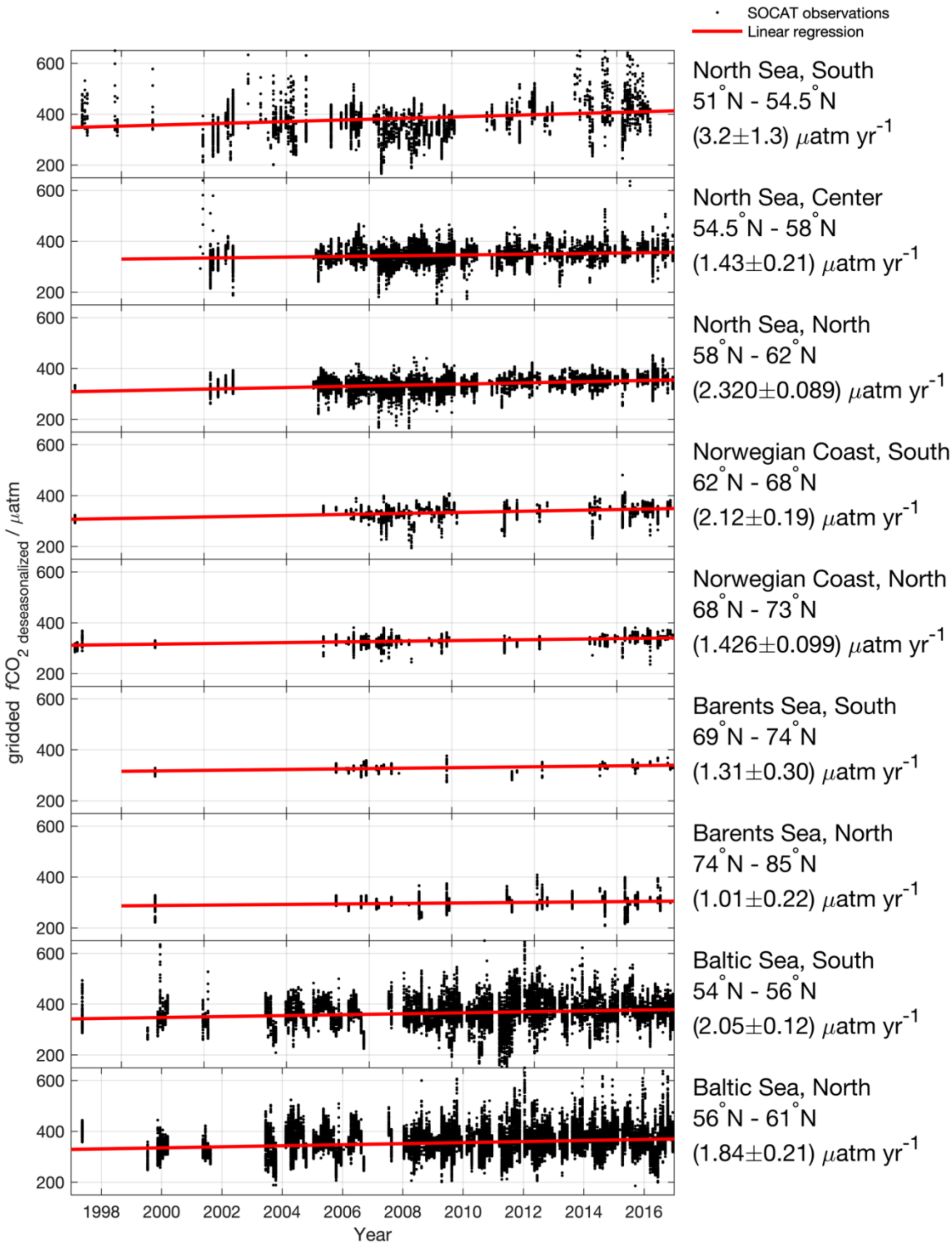

Figure 2: Trend in surface ocean fCO_2 in deseasonalized, gridded observation data (SOCAT v5).

Figure 9 shows that in the Southern bight of the North Sea (<53_N) there's a very strong difference between the part along the UK coast (red color = strong increase of pCO2 in time) and the part along the Dutch coast (blue color = very low increase of pCO2 in time). The two regions are clearly separated along a line that seems to correspond approximately to the 2_ meridian. This line seems to also separate the Central and Northern North Sea although the differences in pCO2 trends are not as marked. But this is really strange as the spatial pCO2 distributions in the Southern Bight of the North Sea are relatively homogeneous horizontally (Thomas et al. 2004; Schiettecatte et al. 2007) so it's really odd that the temporal trends should be so different. This seems to be related to the way the MRL was implemented in the North Sea that seems to have been divided into East and West regions (along the 2_ meridian) in the computation scheme (I guess). Anyway this needs to be addressed, either change the computation scheme to avoid this spatial artefact, or if this is "real" then please provide an explanation for this odd looking spatial difference.

These lines are a remnant of the open ocean pCO2 maps, which were used as a driver in the MLR (in this case Rödenbeck, 4x5° resolution).

> As most the driver data has a smaller resolution than the final maps (see Table3) the grid of the driver data is still visible in the final maps. This is specifically the case for the used open ocean pCO$_2$ maps. Residuals of the original open ocean Rödenbeck map (resolution 5 x 4) are clearly visible in the MLR 1 maps as well as the trends and fluxes calculated from these.

MODERATE COMMENTS

P2 L9 : "small currents caused by the topography" does not cover the full spectrum and complexity of physical processes in continental shelves. In continental shelves there are difference buoyancy sources (thermal and haline stratification) and mixing processes (tides, upwelling, internal waves) that lead to contrasted physical settings. Please refer to classical paper by Blanton (1991).

We agree that in coastal regions more diverse physical processes involved. The processes we named was meant as examples. However, we changed the sentence and added a reference to Blanton (1991).:

> Small scale circulation patterns governed by topographic features, thermal and haline stratification, or mixing though tidal cycles, upwelling or internal waves result in a need for more complex maps with a higher resolution (Bricheno et al., 2014; Lima et al., 2012; Blanton, 1991)

P2 L5-14 : The introduction on the differences between coastal and open ocean waters seems to miss some important elements. CO2 patterns in costal environments are more complex that in the open ocean because overall coastal waters are more productive than open ocean, because there are several sources of nutrients such as mixing processes at continental margins (upwelling and internal wave mixing) and riverine estuarine inputs. In addition shallow areas are vertically mixed while deeper areas are seasonally stratified. Please refer to classical paper of Wollast (1998). Overall this leads to important spatial heterogeneity and strong horizontal gradients of productivity that are reflected in equivalent gradients in surface CO2.

We agree completely with RW1 that the description of differences between open ocean and coastal regions was lacking some of the biogeochemical characteristics. We changed the paragraph accordingly:

> Generally, coastal regions show a larger productivity than open ocean regions due to different additional sources of nutrients (e.g. mixing at continental margins, river runoff). While deeper regions are seasonally stratified, shallow regions are vertically mixed allowing for exchange between the benthic and pelagic parts of the ecosystem (Griffiths et al.,2017, Wollast,1998). Together with strong gradients of productivity this leads to spatial and temporal heterogeneity in surface CO_2 content.

P2 L 15 : Please briefly explain why methods for open ocean are inadequate for coastal waters and provide references if available.

We do not state that the methods are not suitable for coastal oceans. The work of (Laruelle et al., 2017) for example is based on the SOM-FFN method of (Landschützer et al., 2017). Our point is that the currently existing open ocean maps have a too scarce resolution and therefore cannot be used in coastal regions (This is stated in the text). Recently, many reanalysis products that are used as driver variables became available in a higher resolution. In addition to that, the computers get stronger and stronger. This now enables the production of maps with a higher resolution. (At least in regions with sufficient pCO2 observations)

P 3 L 20 : define "winter season" in the southern north sea diatom blooms can start as early as February.

We added the information, which months were used in the respective literature studies to Table 1.
We discuss at different places throughout the manuscript that the variability of spring bloom start, especially in coastal regions, is one of the major limitations of using winter-only trend estimates in coastal regions. In the new version of the manuscript there will be a new paragraph in the discussion section focusing the influence of the season on the trend estimate.

P8 L 13 Nondal et al. (2009) report a TA-salinity relation for the Northern North Atlantic Ocean that should be applicable for Norwegian coast and Barents sea but it could useful to check if it is applicable in the North Sea (e.g. Salt et al. 2013), and in particular in the Southern North Sea (Hoppema et al. 1990).

We agree with RW1 that using the (Nondal et al., 2009) equation results in larger uncertainties in the North Sea, especially the southern North Sea than at the Norwegian Coast or in the Barents Sea. Using Nondal et al equation in the North Sea will most likely result in underestimating the alkalinity at low salinities. In the North Sea the low salinity water usually come either from the Baltic Sea of riverine input. The regressions shown in (Salt et al., 2013) and (Omar et al., 2019) show a larger intercept than the equation we used. Both regressions are focusing on the Skagerrak region and the Northern North Sea The work of (Hoppema, 1990) in the Southern North Sea and the Wadden Sea shows in general very high alkalinity vs salinity ratios compared to the other two studies.
Besides the Skagerrak, regions with low salinity can be found close to shore and at the big river mouths. When looking on the GLODAP dataset alkalinity and salinity in these regions is not correlated at all. Therefore, the pH in these regions should be handled with care. However, for the majority of the North Sea where the salinity is varying between 34 and 35, the equation of Nondal et al describes the salinity-alkalinity correlation better than the equations of Salt et al and Omar et al, which are based on the Baltic Sea inflow. We agree, that using different equations for the different regions could be a good way to improve pH maps based on fCO2 maps in the future.

P 13 L 9-10 : Calling this comparison "validation" is a bit surprising. The authors used the SocatV5 data to generate a fCO2 data using MLR and then compare it again to the original SocatV5 data. This is not a real validation.

We do compare our maps against independent data. We predict our maps for the years 2017 and 2018 and compare these against SOCAT data from these years (SOCATv2019). However, as this obviously is not stated clearly enough, we changed the introduction of this section.

> The prediction of the maps into the years 2017 and 2018 will be compared with data from the newest SOCAT release (SOCATv2019) to have a comparison with an independent dataset.

We added also a sentence to the data handling section:

> A newer version of the SOCAT database (SOCATv2019) was used for validating the maps against independent data.

We acknowledge that the naming of the section 'Validation' caused confusion and changed its name to 'Performance'.

P14L8 you discuss data in 2017 and 2018 but at the end of the introduction (P4L3) you say that you look at trends from 1998 to 2016.

We use the data from 2017 and 2018 for validating our maps. The trends are calculated only until 2016. We did not calculate trends for the latter years, as these have a higher uncertainty due data from these years not being included in the fits. For extending the fits to 2018, we recommend obtaining a new fit equation that includes data from 2017 and 2018. The general goal of these maps is an annual release of the maps based on the latest SOCAT version.

P18L4: Paper of Sharples covers the period 1974 and 2003, so it's a stretch to assume that the trend for the 1974-2003 was continued over the period of 1998 to 2016. There are several other papers that have addressed recent changes of phytoplankton phenology in the North Sea.

We added (Desmit et al., 2020) as a reference. The paragraph was changed to:_

> The bloom timing and onset in the North Sea after the 1990s has been shown to be mainly triggered by the spring-neap tidal cycle and the air temperature (Sharples et al., 2006). The bloom timing and onset was found to be significantly earlier in the 2010s compared to the previous decades (Desmit et al., 2019).

P20L6: "The lower trend stems most likely from an earlier onset of spring bloom" The authors have the data to test this, since they have reconstructed a temporally resolved data-set. If the onset of the bloom is earlier in the year, then so should the peak of the bloom. The seasonal CO2 minimum is a good proxy for peak spring phytoplankton, so the authors can check if this has changed in time and occurred earlier in the year.

We tested this and found the low trends to come mainly from spring (see Figure above). When plotting the seasonal cycles for pCO2 in the early part of the time series in comparison to the later part of the time series, there is a shift to an earlier decrease in pCO2 during spring visible. We think that this is a very interesting topic and it certainly holds the potential for further, more detailed investigation. However, we also think that this will go beyond the aim of this manuscript.

P20L24: "The sea-air CO2 fluxes (Figure 12) show that most regions are a net and increasing sink for CO2. The only source net regions are the southern North Sea and the Baltic Sea. The two different regimes in the North Sea with the southern, nonstratified part being a source and the northern temporarily stratified part a sink for CO2, are well described in the literature (Thomas et al., 2004)." Thomas et al. (2004) only sampled the North Sea during 4 cruises, and their "spring" cruise was in mid-May, when the spring phytoplankton in the Southern Bight of the North Sea is over. So Thomas et al. (2004) missed the peak of the spring bloom (and minimum of CO2) that occurs in April, as clearly shown by the work of Schiettecatte et al. (2007) and Omar et al. (2010). This is why Thomas et al. (2004) reported the Southern Bight of the North Sea as a source of CO2 to the atmosphere, since their data-set does not represent the period of strong CO2 under-saturation during spring. The better seasonally resolved data-set of Schiettecatte et al. (2007) shows in fact that the Southern Bight of the North Sea is a small sink of atmospheric CO2, although admittedly lower than the Northern North Sea.

We do not agree that different timing is the reason why (Schiettecatte et al., 2007) reports the southern North Sea as a sink for CO2, while (Thomas et al., 2004) find it being a source. All spring cruises in (Schiettecatte et al., 2007) were very late in the month. 11BE20040329 and 11BA20040524 are in the SOCAT database. As the paper states that there was a time difference of 28 days between the March,

April and May cruises, respectively, we can assume that the April cruise also took place during the last days of April. That means that the May cruise in (Thomas et al., 2004) (64PE2002506) started only a week after Schiettecatte et al.'s April cruise. (Thomas et al., 2004) might have missed the minimum, but we doubt that this effect is large enough. We think the difference in the various flux estimates is largely driven by interannual variability. As you can see from the data presented in (Omar et al., 2010) bloom timing and intensity can vary rapidly from year to year. Another large factor in comparing these flux estimates is the used wind velocities. Both studies (Schiettecatte et al., 2007 and Thomas et al., 2004) use wind velocity during the time of the cruise. This means the in Schiettecatte et al., (2007) wind data from a few days in the end of the month is used for reporting a monthly flux.
We extended the discussion about this point:

> The sea-air CO_2 fluxes show that most regions are a net and increasing sink for CO_2. The only source net regions are the southern North Sea and the Baltic Sea. The two different regimes in the North Sea with the southern, nonstratified part being a source and the northern temporarily stratified part a sink for CO_2, have been described in the literature before (Thomas et al., 2004). However, there is a large interannual variability in the f CO_2 disequilibrium (Omar et al., 2010). This is reflected in the fact that studies based on different years find conflicting results regarding the direction of the flux (Schiettecatte et al, 2007, Thomas et al., 2004). This large interannual variability can also be found in our maps. During some years larger parts of the North Sea were a net source, while during other years also the southern North Sea acted as net sink.

MINOR COMMENTS

The text contains several typos and inadequate terminology.

We carefully read through the text again and corrected it.

P 2 L 5 : terms like coastal seas, coastal seas or continental shelves would be more adequate than "coasts"

We went through the text and changed the general term coasts to coastal seas or continental shelves

P8 L 12 : "calculating ocean acidification" is an awkward expression. You calculated pH from which you compute a trend. This trend is not necessarily negative (acidification). In some coastal areas an increase of pH has been reported, in other areas there is no trend (Duarte et al. 2013).

We changed 'calculating ocean acidification' to 'calculating pH'.

P 8 L16: "river moths" => river mouths

changed

P19L4: "eutrification" => eutrophication

changed

Legend of Figure 4. Is incorrect. The figures show deltafCO2 not fCO2

changed

P17L8 : "to validate this to validate this"

corrected

P19L5 : Can you provide a reference showing the effect of eutrophication on CO_2 ?

Added references here

References:

Desmit, X., Nohe, A., Borges, A.V., Prins, T., Cauwer, K.D., Lagring, R., Zande, D.V. der, Sabbe, K., 2020. Changes in chlorophyll concentration and phenology in the North Sea in relation to de-eutrophication and sea surface warming. Limnology and Oceanography 65, 828–847. https://doi.org/10.1002/lno.11351

Hoppema, J.M.J., 1990. The distribution and seasonal variation of alkalinity in the Southern Bight of the North Sea and in the Western Wadden Sea. Netherlands Journal of Sea Research 26, 11–23. https://doi.org/10.1016/0077-7579(90)90053-J

Landschützer, P., Gruber, N., Bakker, D.C.E., 2017. An updated observation-based global monthly gridded sea surface pCO_2 and air-sea CO_2 flux product from 1982 through 2015 and its monthly climatology (NCEI Accession 0160558). Version 2.2.

Laruelle, G.G., Landschützer, P., Gruber, N., Tison, J.-L., Delille, B., Regnier, P., 2017. Global high-resolution monthly pCO_2 climatology for the coastal ocean derived from neural network interpolation. Biogeosciences 14, 4545–4561. https://doi.org/10.5194/bg-14-4545-2017

Nondal, G., Bellerby, R.G.J., Oldenc, A., Johannessena, T., Olafssond, J., 2009. Optimal evaluation of the surface ocean CO_2 system in the northern North Atlantic using data from voluntary observing ships. Limnol. Oceanogr. 7, 109–118.

Omar, A.M., Olsen, A., Johannessen, T., Hoppema, M., Thomas, H., Borges, A.V., 2010. Spatiotemporal variations of fCO_2 in the North Sea. Ocean Sci. 13.

Omar, A.M., Thomas, H., Olsen, A., Becker, M., Skjelvan, I., Reverdin, G., 2019. Trends of Ocean Acidification and pCO_2 in the Northern North Sea, 2003–2015. Journal of Geophysical Research: Biogeosciences 124, 3088–3103. https://doi.org/10.1029/2018JG004992

Salt, L.A., Thomas, H., Prowe, A.E.F., Borges, A.V., Bozec, Y., Baar, H.J.W. de, 2013. Variability of North Sea pH and CO_2 in response to North Atlantic Oscillation forcing. Journal of Geophysical Research: Biogeosciences 118, 1584–1592. https://doi.org/10.1002/2013JG002306

Schiettecatte, L.-S., Thomas, H., Bozec, Y., Borges, A.V., 2007. High temporal coverage of carbon dioxide measurements in the Southern Bight of the North Sea. Marine Chemistry, Special issue: Dedicated to the memory of Professor Roland Wollast 106, 161–173. https://doi.org/10.1016/j.marchem.2007.01.001

Thomas, H., Bozec, Y., Elkalay, K., Baar, H.J.W. de, 2004. Enhanced Open Ocean Storage of CO_2 from Shelf Sea Pumping. Science 304, 1005–1008. https://doi.org/10.1126/science.1095491

Answer to Reviewer 2

(reviewer comment, author response, change in manuscript)

This is an interesting manuscript that tackles an important problem: maps interpolating sparse observations of surface ocean pCO_2 (and related variables like pH) perform well in the open ocean but generally do not accurately reproduce the conditions seen in more complex shelf sea environments like the northwest European continental shelf, the focus of this study. The authors apply a long-established technique (MLR) but with the innovative step of using low-resolution open-ocean pCO_2 maps as one of the predictors. They tested two different open-ocean pCO_2 maps and also developed a 'traditional' MLR based only on other in situ variables. One of the open-ocean maps, which did project pCO_2 values across the shelf seas, performed slightly better than the traditional MLR but the other, which did not, performed better or worse depending on the metric considered, although the authors state it was better. The former open-ocean-map-based MLR was therefore used to derive most of the results. The discussion is mostly a description of the trends in surface ocean pCO_2, air-sea CO_2 fluxes and pH in the relevant shelf seas.

There are a few issues I think the authors should consider revising before publication: One of the strongest reasons to use an MLR instead of a neural network approach is the relative ease with which the predictive model can be shared and used by other researchers. Please would the authors therefore provide the actual fitted coefficients to their equation 1.

We recommend strongly to develop a specific fit for any new application. The fit coefficients are expected to change with using different products of driving data. Additionally, the driving data products are updated and improved regularly. As these annual updates often also involve changes in the historic data a new fit should be done for any new combination of driver data.

The word 'coasts' is used throughout to describe the study area but it is not clear how this is defined. For me 'coast' would refer to the very near coastal zone (e.g. intertidal areas) as opposed to 'shelf sea' which would go out to a depth contour of e.g. 200 m. The results do not also extend all the way to the coast, as can be seen from the white gaps between land and ocean on Figures 4, 5, and 9–12 and noted in the penultimate sentence of the Conclusions. Please explicitly define, and consider revising, the terminology used.

We changed the use of the very general term coasts to coastal seas or continental shelves. The definition for coastal seas as used in this work can be found under Methods: Study area. A limiting factor for the extension of the maps to land is the availability of driver data. Intertidal areas for example are not represented in the driver data. We also added a sentence in the section 'Methods: Study area' to clarify what we mean when we use the term coastal seas in this manuscript.

> Please note, that this study concentrates on the continental shelf area. the near coastal zones (e.g. intertidal zones) are not included due to the limited availability of driver data in these regions.

Is it valid to predict all the way up into the northern Baltic Sea given that there appears to be only one month of data there (Figure 2)?

This is a good question. One could easily argue to remove this part. We decided to include it to give a flux estimate for the entire Baltic Sea. Within ICOS, there was a new underway pCO2 system installed on a commercial vessel sailing through the Gulf of Bothnia in 2019. We therefore expect a much better data coverage in the region from 2019 on. It will be very interesting to compare the maps we show here with an updated version that include a full annual cycle in the Gulf of Bothnia.

The previous study results given in Table 1 for the North Sea show a range of different values (specifically, Thomas et al. (2007) vs Salt et al. (2013)) and also covering different time periods, with Salt et al. finding a different rate of change from 2001- 2005 compared with 2005-2008. Salt et al.

implicate the NAO as a key driver of this short-term variability, but this study does not mention the NAO explicitly. Do these new results provide any evidence for the NAO influencing air-sea CO_2 exchange here? On the other hand, Figure 9, upper left grid box panel for the North Sea, indicates that no significant trend can be found in the North Sea for these short periods reported by previous studies. Implicitly, this figure is therefore saying that the different trends reported in previous studies are in fact not significant. Is that a point the authors intend to make? Either way it feels like there is some interesting discussion missing here.

We think that in depth testing of underlying drivers, such as NAO, is exceeding the aim of this manuscript. Here, we primarily want to present the maps. That being said, we did of course have a look at potential driving factors, but we did not find evidence for the NAO to be a key driver in any of the regions. When looking into detail there are a few features that seem to be related (such as for example the large disequilibrium in the Norwegian Coast region in 2010, a year with a very negative NAO index).

p19, line 1 states the western North Sea did not show a significant trend, but this area does not have black dots in Figs 9 and 10. Are trends significant here or not? Also, this paragraph as a whole does not effectively justify or explain its opening sentence.

We changed this sentence to:

> The observation that large subareas (the Baltic Sea, along the shore of the western North Sea) did not show a significant trend can be explained by the fact, that coastal sea systems, especially enclosed areas as the Baltic Sea, experience a high anthropogenic pressure.

Please provide details of all CO2SYS options selected (e.g. borate:chlorinity). Consider using the newer CO2SYS v2 from Orr et al. (2018) and including error propagation from the equilibrium constants in your calculations?

Added the information about the boron-salinity ratio. We are working on including the error propagation into our scripts and this will be included in a future, updated release of the maps.

Finally, a few minor points to consider:
It is noted several times that and old version of SOCAT (v5) was used for the fitting before the explanation on p8 that the reason for this was so that the newer version could be used to independently test the fits. It would be helpful to mention this the first time SOCAT is discussed.

The possibility to compare was one point and the other was the time that past when preparing and analyzing the maps. We added the following sentence to the 'data handling' section:

> A newer version of the SOCAT database (SOCATv2019) was used for validating the maps against independent data.

Why do the different panels in Figure 3 (in particular the second panel) show different subsets of SOCAT data points?

changed

Figure 4: colour bar should be labelled fCO_2, not _fCO_2.

changed

Figures 5, 9, etc.: maps contain a lot of straight lines and right angles, usually indicates boundaries between regions with different predictive equations but they don't entirely match with the regions shown in Figure 1, what is the cause?

These lines are an artifact stemming from the open ocean pCO2 maps that were used as a driver. You can see here the remains of the 4x5 ˚ grid of the original Rödenbeck et al product.

Figure 9: what is the difference between a cross and a circle?

Significant increase/decrease of temperature with time. This is described both in the figure itself, as in the figure description.

The colour scale on Figure 11 feels counterintuitive, as usually CO_2 source areas are shown in red and sinks in blue.

Changed the color code in Figure 11 and 12

p9 line 2: missing citation.

Added reference

p10 line 3: MLR, not MLD.

changed

In units for rates please explicitly clarify whether d means decade or day.

The unit of all rates shown in this manuscript is per year. It is the unit of the fluxes is per day. We do not see the need for clarification here.

There are a few issues with the English language throughout so this aspect should also be carefully checked through.
I support the comments and suggestions made by the other reviewer.

The northern European shelf as increasing net sink for CO_2

Meike Becker[1,2], Are Olsen[1,2], Peter Landschützer[3], Abdirhaman Omar[4,2], Gregor Rehder[5], Christian Rödenbeck[6], and Ingunn Skjelvan[4,2]

[1]Geophysical Institute, University of Bergen, Bergen, Norway
[2]Bjerknes Center for Climate Research, Bergen, Norway
[3]Max Planck Institute for Meteorology, Hamburg, Germany
[4]NORCE Norwegian Research Centre AS, Bergen, Norway
[5]Leibniz Institute for Baltic Sea Reasearch, Warnemünde, Germany
[6]Max Planck Institute for Biogeochemistry, Jena, Germany

Correspondence: Meike Becker (meike.becker@uib.no)

Abstract. We developed a simple method to refine existing open ocean maps and extending them towards different coastal seas. Using a multi linear regression we produced monthly maps of surface ocean fCO_2 in the northern European coastal seas (North Sea, Baltic Sea, Norwegian Coast and in the Barents Sea) covering a time period from 1998 to 2016. A comparison with gridded SOCAT v5 data revealed standard deviations ~~of the residuals~~ and residuals of $0{\pm}26\mu$atm in the North Sea, $0{\pm}16\mu$atm along the Norwegian Coast, $0{\pm}19\mu$atm in the Barents Sea, and $2{\pm}42\mu$atm in the Baltic Sea. We used these maps as basis to investigate trends in fCO_2, pH and air-sea CO_2 flux. The surface ocean fCO_2 trends are smaller than the atmospheric trend in most of the studied ~~region. Only~~ regions. Only in the western part of the North Sea ~~is showing~~ we found an increase in fCO_2 close to 2 μatm yr^{-1}, which is similar to the atmospheric trend. The Baltic Sea does not show a significant trend. Here, the variability was much larger than ~~possibly observable~~ the expected trends. Consistently, the pH trends were smaller than expected for an increase of fCO_2 in pace with the rise of atmospheric CO_2 levels. The calculated air-sea CO_2 fluxes revealed that most regions were net sinks for CO_2. Only the southern North Sea and the Baltic Sea emitted CO_2 to the atmosphere. Especially in the northern regions the sink strength increased during the studied period.

Copyright statement. TEXT

1 Introduction

For facing global challenges, such as predicting and tracking climate change, it is important to improve our understanding of the ocean carbon sink and its variability. Open oceans, especially those of the northern hemisphere, are relatively well understood and described in their large-scale variability (Gruber et al., 2019; Landschützer et al., 2018, 2019; Fay and McKinley, 2017). Reliable autonomous systems for measuring carbon dioxide partial pressure from commercial vessels were developed in the early 2000s (Pierrot et al., 2009) and have since been deployed on a large number of vessels (e.g. (Bakker et al., 2016). This has resulted in sufficient data to develop methods to interpolate the data and to describe large scale air-sea CO_2 exchange and its variability (Landschützer et al., 2014, 2013; Rödenbeck et al., 2013; Jones et al., 2015). These methods cover a wide variety of approaches, such as linear interpolations, machine learning, and model based estimates. By comparing the different results it is possible to achieve a good estimate of the uncertainty associated with the respective methods and to evaluate their performance relative to each other (Rödenbeck et al., 2015).

Despite coasts coastal seas cover 7-10% of the world's oceans (Bourgeois et al., 2016), their contribution to the oceanic carbon sink is not yet fully constrained. Whether coastal oceans seas are a net sink or source for atmospheric CO_2 and how their role will change in a changing climate is still under debate (Bauer et al., 2013; Laruelle et al., 2010). Compared to the open ocean, longer time series and a higher spatial and temporal resolution of the observations are needed in order to capture all relevant coastal processes. Circulation patterns such as small currents caused by the topography, or tidal cycles Small scale circulation patterns governed by topographic features, thermal and haline stratification, or mixing through tidal cycles, upwelling or internal waves result in a need for more complex maps with a higher resolution (Bricheno et al., 2014; Lima and Wethey, 2012 (Bricheno et al., 2014; Lima and Wethey, 2012; Blanton, 1991). These physical drivers are not the only reasons for coasts coastal seas being more complicated to understand. Processes taking place in the sediments or respiration of sinking material do not directly affect the surface in the open ocean . In shallow coastal regions the water column can easily be mixed all the way to the bottom allowing for echange Generally, coastal regions show a larger productivity than open ocean regions due to different additional sources of nutrients (e.g. mixing at continental margins, river runoff). While deeper regions are seasonally stratified, shallow regions are vertically mixed allowing for exchange between the benthic and pelargic pelagic parts of the ecosystem (Griffiths et al., 2017). (Griffiths et al., 2017; Wollast, 1998). Together with strong gradients of productivity this leads to spatial and temporal heterogeneity in surface CO_2 content.

The different maps developed for describing the open ocean surface $p$$CO_2$ (CO_2 partial pressure) dynamics and air-sea CO_2 fluxes are not directly suitable for use the application in coastal regions. Many exclude data from coastal regions continental shelves completely while all of them have a too coarse spatial resolution to properly resolve the coast with its small-scale variability (typically between 1 and 5 °) to properly resolve coastal seas with their small-scale variability. A few studies tried to describe coastal carbon dynamics but most of them had have strong regional or temporal limitations. Table 1 shows an overview of studies with estimated $p$$CO_2$ trends over the northern European shelf while Table 2 presents available flux estimates. Laruelle et al. (2017) used a neural network approach to produce a global $p$$CO_2$ climatology of coastal oceansseas, describing more distinct seasonal variability in the northern hemisphere than in the southern Pacific and Atlantic. Few studies attempted to constrain coastal air-sea fluxes before. Laruelle et al. (2018) published trend estimates in regions with a high data coverage based on winter data spanning up to 35 yearsfinding . They find the $p$$CO_2$ rise in coastal regions to lag behind the atmospheric rise in CO_2. For the Baltic Sea, Parard et al. (2016, 2017) used a neural network approach to produce surface ocean $p$$CO_2$ maps from 1998 to 2011 and estimated an air-sea flux of 1.2 mmol m^{-2} day^{-1}. Yasunaka et al. (2018) estimated a flux of 8 - 12 mmol m^{-2} day^{-1} in the Barents Sea and along the Norwegian coast using a self-organizing map technique. Most of the other available studies on the trends in coastal $p$$CO_2$ are based on data from either summer or winter. Estimates based on summer-only data typically show large interannual variations (Thomas et al., 2007; Salt et al., 2013), which led to the conclusion that here the interannual variability masks the actual long term trend. The approach to use winter-only data (Fröb

Table 1. Overview of trends in surface ocean CO_2 reported in the literature.

	Reference	Time range	$dpCO_2/\,dt$ / μatm yr^{-1}
North Sea	Thomas et al. (2007)	2001-2005, summer data normalized to 16°	7.9
North Sea	Salt et al. (2013)	2001-2005, summer data, normalized to 16°	6.5
North Sea	Salt et al. (2013)	2005-2008, summer data, normalized to 16°	1.33
Faeroe Banks	Fröb et al. (2019)	2004-2017, winter data (DJFM)	2.25 ± 0.20
North Sea, west	Omar et al. (2019)	2004-2017, winter data (DJ)	2.19 ± 0.55
North Sea, east	Omar et al. (2019)	2004-2017, winter data (DJF)	not significant
North Sea	Laruelle et al. (2018)	1988-2015	almost no trend
English channel	Laruelle et al. (2018)	1988-2015	slightly smaller than atmosphere
Baltic Sea	Wesslander et al. (2010)	1994-2008	larger than atmosphere
Baltic Sea	Schneider and Müller (2018)	2008-2015	4.6 - 6.1
Baltic Sea, west	Laruelle et al. (2018)	1988-2015	much smaller than atmosphere, slightly negative
Barents Sea	Yasunaka et al. (2018)	1997-2013	not significant
Barents Sea	Laruelle et al. (2018)	1988-2015	about the same as atmosphere
Atmosphere	global average	1997-2016	2.02 ppm yr^{-1}

Table 2. Overview of air-sea CO_2 fluxes reported in the literature. Negative sign denotes flux from atmosphere to ocean.

	Reference	Time range	F / mmol m^{-2} day^{-1}
North Sea	Meyer et al. (2018)	2001/2002	-3.8
Baltic Sea	Parard et al. (2017)	1998-2011	1.2
Norwegian Coast	Yasunaka et al. (2018)	1997-2013	-4 - -8
Barents Sea	Yasunaka et al. (2018)	1997-2013	-8 - -12

et al., 2019; Omar et al., 2019), on the other hand, is based on the assumption that during this season the influence of biological processes is negligible and therefore winter data can be used to establish a baseline trend. However, also using winter-only data has its drawbacks. In particular the choice of which months to include can cause biases and the optimal selection can differ from region to region .

In this study we present a new approach to develop monthly fCO_2 (CO_2 fugacity) maps based on already existing open ocean pCO_2 maps, in four example regions: North Sea, Baltic Sea, Norwegian Coast and the Barents Sea, with the aim to determine the air-sea CO_2 exchange in these regions and its decadal trends. A multi linear regression (MLR) was used , fitting to fit driver data against fCO_2 observations. Based on the resulting fCO_2 maps and a salinity-alkalinity correlation we also produced monthly maps of coastal pH. The performance of the produced maps was evaluated and the maps were then used to investigate trends in coastal fCO_2 and pH in the entire region from 1998 to 2016. Finally, we calculated used the fCO_2 maps to determine the air-sea CO_2 fluxes and show their exchange and show its temporal and spatial patterns. ß

2 Method

2.1 Study area

This work focuses on northern European coasts the northern European continental shelf and marginal seas. As we want to show the performance of the MLR method we picked a number of regions with very different characteristics: the North Sea, the Baltic Sea, the Norwegian coast and the western Barents Sea (Figure 1). We decided to concentrate on these regions specifically because (1) the data coverage in these regions is fairly high and (2) the authors have strong knowledge on the specific regions. This is important in order to properly evaluate the maps and to assess whether or not the output is realistic. The 4 four regions were defined based on the COastal Segmentation and related CATchments (COSCAT) segmentation scheme (Laruelle et al., 2013). The threshold for defining a region as coastal sea was set to a depth limit of 500 m(Figure 1). By using this definition, we produce an overlap to the open ocean maps, allowing our maps to be merged with the open ocean maps. Please note, that this study concentrates on the continental shelf area. the near coastal zones (e.g. intertidal zones) are not included due to the limited availability of driver data in these regions.

2.2 Data handling

The CO_2 data used in this study were extracted from SOCAT version 5 (Bakker et al., 2016). Their coverage is shown in Figure 2. A newer version of the SOCAT database (SOCATv2019) was used for validating the maps against independent data. An overview over the reanalysis products used as driver data is given in Table 3. We use as basic driver data sea surface temperature (SST), sea surface salinity (SSS), chlorophyll a concentration (Chl a), mixed layer depth (MLD), bathymetry (BAT), distance from shore (DIST), ice concentration (ICE), the change in ice concentration from month to month. Chl a values during the dark winter season were set to 0. In addition to the reanalysis data, pCO_2 values from the closest coastal grid cell of the open ocean map was were used as a driver in our MLR. We can neglect the difference between partial pressure and fugacity of CO_2 (about 1 μatm) at this place as it is much smaller than the accuracy of the data extracted from SOCAT v5 (2 to 10 μatm) and the uncertainty associated to the open ocean maps. The open ocean pCO_2 values were extracted from two different products (Rödenbeck et al. (2014) (version oc_v1.5) and Landschützer et al. (2017, 2016) (version 2016)). Rödenbeck et al. (2014) is based on a data-driven diagnostic model of ocean biogeochemistry fitted against surface pCO_2 observations while Landschützer et al. (2016) is based on uses a two-step neural network (a feed-forward network coupled with self-organizing maps, FFN-SOM) trained with the pCO_2 observations. Please note that the Rödenbeck open ocean map also contains data in coastal grid boxes, while the Landschützer open ocean map is restricted to the open ocean regions south of 80°N. The MLR models based on these two are called MLR 1 (based on the coastal pCO_2 values from the Rödenbeck map) and MLR 2

Table 3. Products used as driver data in the MLR and the maps.

Product used	Resolution	Reference
Chl a for MLR	4km x 4km, 8 days	Global Ocean Chlorophyll (Copernicus-GlobColour) from Satellite Observations - Reprocessed
Chl a for maps	4km x 4km, monthly	Global Ocean Chlorophyll (Copernicus-GlobColour) from Satellite Observations - Reprocessed
MLD	12.5km x 12.5km, monthly	Arctic Ocean Physics Reanalysis
ICE	0.25°x0.25°, monthly	Cavalieri et al. (1996)
SST / SSS	0.25°x0.25°, weekly	Global Ocean Observation-based Products Global_Rep_Phy_001_021
BAT	2min x 2min	ETOPO2v2 Center (2006)
Rödenbeck pCO_2	5° x 4°, monthly	Rödenbeck et al. (2014)
Landschützer pCO_2	1° x 1°, monthly	Landschützer et al. (2017)

(based on the the nearest open ocean pCO_2 values of the Landschützer map), respectively. To determine the extent to which the regressions benefit from the information in the open ocean maps, a third MLR, MLR 3, was determined. ~~This does not have~~ Here, we do not use any of the open ocean maps as driver, but instead ~~uses~~ the year as a proxy for the annual rise in CO_2.

For producing the input data for the MLR, each SOCAT fCO_2 data point was assigned to the closest data point in space and time of each of the reanalysis data. This produces a matrix as long as the SOCAT fCO_2 observations for each driver data. After this, the fCO_2 data as well as all driver data were binned on a monthly 0.125°x0.125° grid covering 1998 to 2016. This step ensures that the driver data have the same bias in space and time within each grid box as the fCO_2 data. If a grid box for example only contains observations from the first week of the month and the northwestern corner, we make sure, that also the gridded driver data only contains values from the first week and the northwestern corner of the grid box, and not an average over the entire month and grid box. This is mostly important for the chlorophyll driver data, which are available in a very high resolution compared to the fCO_2 maps produced in this work. These driver data were used for the MLR.

For producing the final maps, a second set of the driver data was produced, in the following called field data. Here the driver data were directly regridded to a monthly 0.125°x0.125° grid, providing the full spatial and temporal coverage and a ~~homogene~~ homogeneous average in each grid box. The field data were used to produce the fCO_2 maps based on the equation derived from the MLR.

2.3 Multi linear regression

The multi linear regression models were constructed by forward and backward stepwise regression using the driver data as predictor variables to model the fCO_2 observations. During a stepwise regression in each step, a variable is tested for being added or removed from the set of explanatory variables. This decision on whether to add or remove a term was based on the p-value of the F-statistic with or without the term in question. The entrance tolerance was set to 0.05 and the exit tolerance to

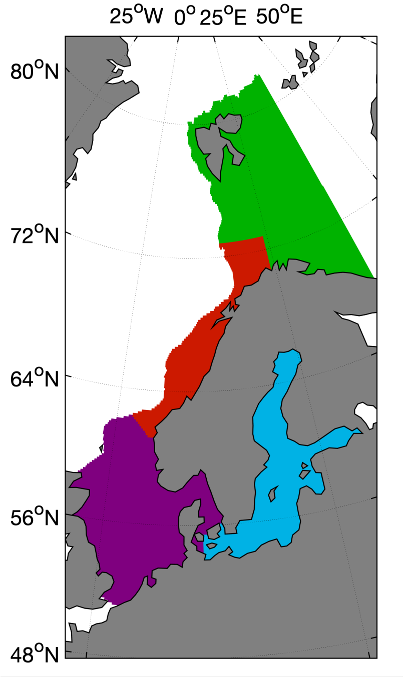

Figure 1. The study area and the location of the four different regions North Sea (purple), Norwegian Coast (red), Barents Sea (green) and Baltic Sea (blue).

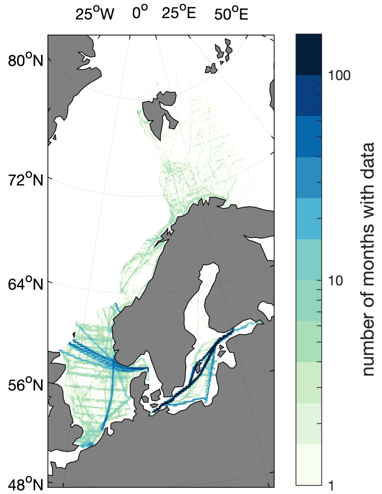

Figure 2. The number of months with $f\mathrm{CO}_2$ data from SOCAT v5 in each grid box.

Table 4. Driver used in the different regressions.

	MLD	SST	SSS	CHL	ICE	ICE change	BAT	DIST	pCO_2	year
North Sea										
MLR 1	x	x	x	x	x		x		x	
MLR 2	x	x	x	x	x	x	x	x	x	
MLR 3	x	x	x	x	x	x	x	x		x
Norwegian Coast										
MLR 1	x	x	x	x	x		x		x	
MLR 2	x	x	x	x	x	x	x		x	
MLR 3	x	x	x	x	x	x	x			x
Barents Sea										
MLR 1	x	x	x	x	x	x	x		x	
MLR 2	x	x	x	x	x	x	x		x	
MLR 3	x	x	x	x	x	x	x			x
Baltic Sea										
MLR 1	x	x	x	x	x	x	x		x	
MLR 2	x	x	x	x	x	x	x		x	
MLR 3	x	x	x	x	x		x			x

0.1. The model includes constant, linear, and quadratic terms as well as products of linear terms. Equation 1 gives the basic equation, with $X_1 ... X_n$ being the driver data and $a_1 ... a_{nn}$ the regression coefficients.

$$y = a_0 + a_1 \cdot X_1 + ... + a_n \cdot X_n + a_{12} \cdot X_1 X_2 + ... + a_{mn} \cdot X_m X_n + a_{11} \cdot X_1^2 + ... + a_{nn} \cdot X_n^2 \tag{1}$$

The pCO_2 value of the respective open ocean maps (MLR 1 and MLR 2), or the year were added (MLR 3). Inclusion of stationary drivers (such as month, latitude and longitude) in the MLR increased the performance of MLR 2 and MLR 3. However, these were still not better than MLR 1 and we therefore decided to limit this analysis to dynamic parameters. Using dynamic drivers only assures a dynamic description of the conditions in the field, and gives us the possibility to reproduce changes caused by a regime shifts, for example the ongoing ~~atlanticfication~~ atlantification of the Barents Sea (Oziel et al., 2016; Lind et al., 2018).

2.4 Validation

The three linear fits were compared to each other by taking into account the R^2 and the root mean square error (RMSE) of the fit, and the Nash Sutcliffe method efficiency (ME) (Nondal et al., 2009). The method efficiency compares how well the model output (E_n) fits the observations (I_n) for every data point n to how well a simple monthly average ($\bar{I}$) would fit the observations:

$$\mathrm{ME} = \frac{\sum_n (I_\mathrm{n} - E_\mathrm{n})^2}{\sum_n \left(I_\mathrm{n} - \bar{\mathrm{I}}\right)^2} \tag{2}$$

A method efficiency >1 means that using just monthly averages of all data in the region would fit better to measured data than the respective model, Generally, a method efficiency >0.8 is considered bad. Besides the statistics of the fit itself, the final maps were also compared to the gridded SOCAT v5 data, resulting in an average offset and standard deviation. In order to compare the maps against data that were not used to produce the maps, we predicted the $f\mathrm{CO_2}$ for the years 2017 and 2018 (ie, we applied the trained multi-linear model to driver data from 2017 and 2018) and compared these maps to $f\mathrm{CO_2}$ observations in SOCAT v2019, gridded on a monthly 0.125°x0.125° grid. We also compare the ~~map~~ maps directly with observations ~~at two~~ from time series in the North Sea and the Baltic Sea.

2.5 Ocean acidification

For calculating ~~ocean acidification~~the pH, alkalinity (AT) was estimated in the North Sea, along the Norwegian Coast, and in the Barents Sea via a salinity-alkalinity correlation after Nondal et al. (2009). Alkalinity describes the capacity of the sea water to buffer changes in pH. As the concentration of most of the weak acids in seawater is strongly dependent on the salinity, alkalinity can in many regions be estimated from salinity. However, in regions with a high amount of organic acids in seawater, for example in strong blooms or at river ~~moths~~mouths, deviations from the alkalinity-salinity relationship can be observed. The carbonate system was calculated using the CO2SYS program (van Heuven et al., 2009) with carbonic acid dissociation constants of Mehrbach et al. (1973) as refitted by Dickson and Millero (1987)~~and~~ , $\mathrm{KSO_4^-}$ dissociation constants after Dickson (1990) and the boron-salinity relation after Uppström (1974). For the Baltic Sea, we did not calculate pH as the alkalinity-salinity relationship in this region is complex due to different AT-S relations in different sub-regions of the Baltic Sea, and a non-negligible increase of AT over the last 25 years (Müller et al., 2016).

2.6 Calculation of trends

For calculating trends of $f\mathrm{CO_2}$ and ocean acidification, the data in every grid box were deseasonalised by subtracting the long-term averages of the respective months. Then a linear fit was applied to the deseasonalised time-series. For illustrating the influence of interannual variability we calculated the trend for different time ranges. As a time range less than 10 years barely resulted in significant trends, we decided to limit the trend analysis to starting years from 1998 to 2006 and ending years from 2008 to 2016.

2.7 Flux calculation

The air-sea disequilibrium was calculated as the difference between our mapped $f\mathrm{CO_2}$ values and atmospheric $f\mathrm{CO_2}$ in each grid cell and time step. The atmospheric $f\mathrm{CO_2}$ was determined by converting the $x\mathrm{CO_2}$ from the NOAA Marine Boundary

Layer Reference product from the NOAA GMD Carbon Cycle Group into $f\mathrm{CO}_2$ by using the monthly SST and SSS data (Table 3) and monthly air pressure data from the NCEP-DOE Reanalysis 2 (?)(Kanamitsu et al., 2002). We calculated the air-sea CO_2 flux (F) according to Equation 3, such that negative fluxes are into the ocean. The gas transfer coefficient k was determined using the quadratic wind speed (u) dependency of Wanninkhof (2014) (Equation 4). The Schmidt number, Sc, was calculated according to Wanninkhof (2014) and the solubility coefficient for CO_2, K_0, after Weiss (1974).

$$\mathrm{F} = k \cdot K_0 \cdot (f\mathrm{CO}_{2,\mathrm{sw}} - f\mathrm{CO}_{2,\mathrm{atm}}) \tag{3}$$

$$k = a_q \cdot \langle u^2 \rangle \cdot \left(\frac{Sc}{660}\right)^{-0.5} \tag{4}$$

In our calculations, we used 6-hourly winds of the NCEP-DOE Reanalysis 2 product. The coefficient a_q in Equation 4 is strongly dependent on the used wind product (Roobaert et al., 2018). We determined it to be $a_q = 0.16\mathrm{cmh}^{-1}$ for the 6-hourly NCEP 2 product following the recommendations of Naegler (2009) and by using the World Ocean Atlas sea surface temperatures (Locarnini et al., 2018). The barrier effect of sea ice on the flux was taken into account by relating the flux to the degree of ice cover following of Loose et al. (2009). As the gas exchange in areas that are considered 100% ice covered from satellite images should not be completely neglected, we use a sea ice barrier effect for a 99% sea ice cover in all grid cells where the sea ice coverage exceeded 99%.

3 Results

3.1 Maps of $f\mathrm{CO}_2$

The skill assessment metrics for MLR 1, MLR 2 and MLR 3 are presented in Table 5. It shows the the R^2 and RMSE of the fit, the ME, as well as the average offset and standard deviation to the gridded SOCAT data. The MLRs substantially improve the predictions of the open ocean maps in all studied regions, showing a better average offset and standard deviation to SOCAT v5 and ME than the coarser-resolution open ocean maps (for example: Rödenbeck map: North Sea 0 ± 95 μatm, Norwegian Coast: 2 ± 17 μatm, Barents Sea: 22 ± 40 μatm, Baltic Sea: 4 ± 48 μatm; MLD1MLR1: North Sea: 0 ± 26 μatm, Norwegian Coast: 0 ± 16 μatm, Barents Sea: 0 ± 19 μatm,Baltic Sea: 2 ± 42 μatm). In all regions MLR 1 was performing best, showing also the best model efficiency, the highest R^2 and the smallest RMSE of the fit, while MLR 2 and MLR 3 showed a weaker performance. This can be explained by the fact that the Rödenbeck map contains also information about the coasts continental shelf and the Barents Sea, while for MLR 2 the closest open ocean grid cell of Landschützer et al. (2017) was used. MLR 3 showed the weakest performance, which shows the value of using information from the open ocean maps in the regression.

Figure 3 shows, from left to right, the spatial distribution of the average difference between the predicted $f\mathrm{CO}_2$ by MLR1 and the gridded SOCAT v5 data, the Rödenbeck map and the gridded SOCAT v5 data, the difference between MLR 1 and the Rödenbeck map, and, for comparison, between MLR 3 and the SOCAT v5 data. In the North Sea, MLR 1 seems to slightly overestimate the $f\mathrm{CO}_2$ in the constantly mixed region at the entrance of the English channel and the area off the Danish North

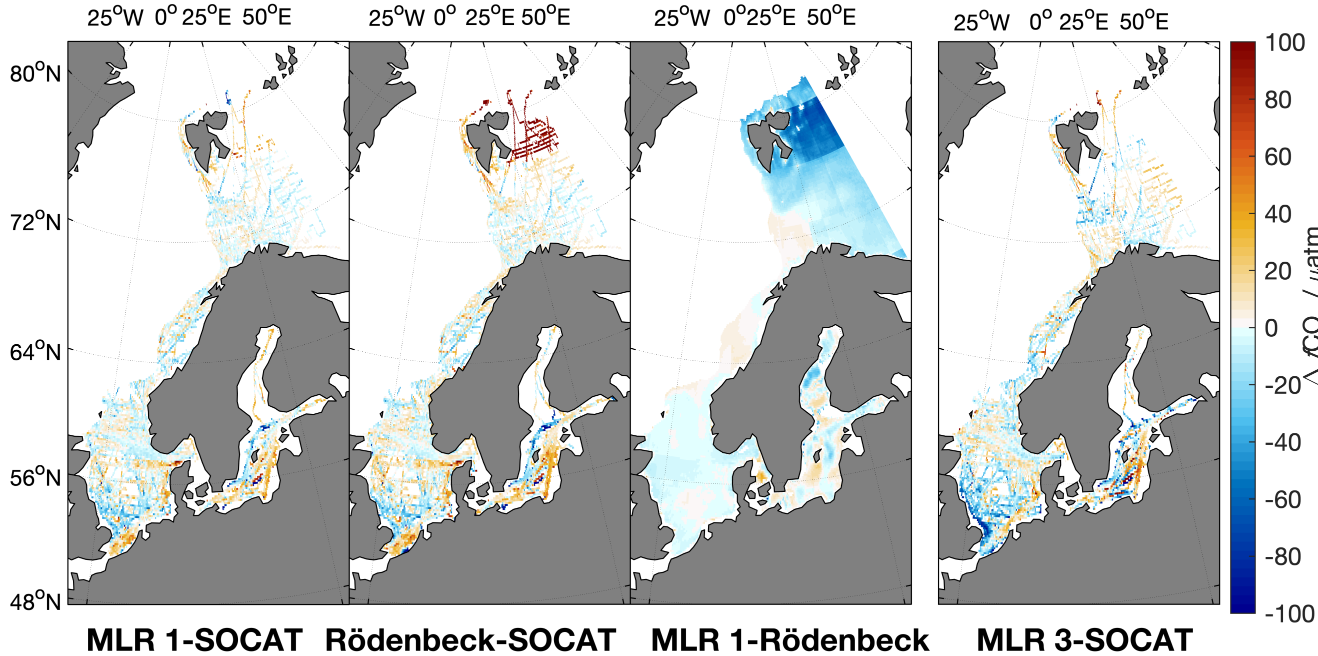

Figure 3. Average regional differences between MLR 1 and gridded SOCAT v5 data, the Rödenbeck map and gridded SOCAT v5 data, MLR 1 and the Rödenbeck map, and MLR 3 and the gridded SOCAT v5 data (from left to right).

Sea coast. In the Baltic, MLR 1 generally describes well the spatial variability in fCO_2. In the Gulf of Finland it usually predicts too low fCO_2 values during May/June while MLR 1 slightly underestimates events of very high fCO_2 in December/January. However, it shows lower spatial biases than the original Rödenbeck map. MLD 2 and 3 are showing much larger differences from SOCAT v5 data, especially in the Baltic Sea and the southern North Sea. Therefore, we will use MLR 1 in the further analysis. An extended validation of the MLR 1 maps can be found in the discussion section.

As most driver data have a smaller resolution than the final maps (see Table 3), the grid of the driver data can be still visible in the final maps. This is specifically the case for the used open ocean pCO_2 maps. Residuals of the original open ocean Rödenbeck map (resolution $5° - 4°$) are clearly visible in the MLR 1 maps as well as the trends and fluxes calculated from these.

Figure 4 shows the monthly averages of fCO_2 produced by MLR 1 for February, May, August and November. In all regions, the highest fCO_2 values occur in the winter, while the lowest fCO_2 occur in summer. The largest seasonal cycle could be observed in the Baltic Sea, where fCO_2 reached well below 200 μatm in mid summer and over 500 μatm during the winter.

Table 5. Statistical evaluation of the MLR 1, MLR 2 and MLR 3 in comparison to the open ocean maps of Rödenbeck et al. (2015) and Landschützer et al. (2017) for each region. The data for the open ocean map of Landschützer et al. (2017) are in parentheses since this is based on an extrapolation of he closed open ocean grid cell towards the coast. The number of grid cells containing data is given behind the region abbreviations.

	R^2 adj	RMSE	ME	difference to gridded SOCAT v5	
			median	mean	standard deviation
		/μatm		/μatm	/μatm
North Sea (36170)					
MLR 1	0.7271	25	0.3145	-0.15	26
MLR 2	0.5130	33	0.5789	-0.52	36
MLR 3	0.5331	33	0.4895	-2.4	32
Rödenbeck			0.3522	-0.28	95
(Landschützer)			0.5714	-4.7	103
Norwegian Coast (16014)					
MLR 1	0.7860	16	0.1742	0.46	16
MLR 2	0.5634	22	0.3597	-2.3	24
MLR 3	0.6074	20	0.2436	-0.08	21
Rödenbeck			0.2177	2.0	17
(Landschützer)			0.3294	7.0	23
Barents Sea (13925)					
MLR 1	0.8871	12	0.1069	0.32	19
MLR 2	0.8724	14	0.0986	1.3	68
MLR 3	0.8672	18	0.1082	1.3	24
Rödenbeck			0.2923	22	40
(Landschützer)			0.3364	15	44
Baltic Sea (46810)					
MLR 1	0.9076	39	0.0488	2.2	42
MLR 2	0.6733	66	0.3111	-1.0	68
MLR 3	0.6628	67	0.3027	0.24	69
Rödenbeck			0.1326	4.2	48

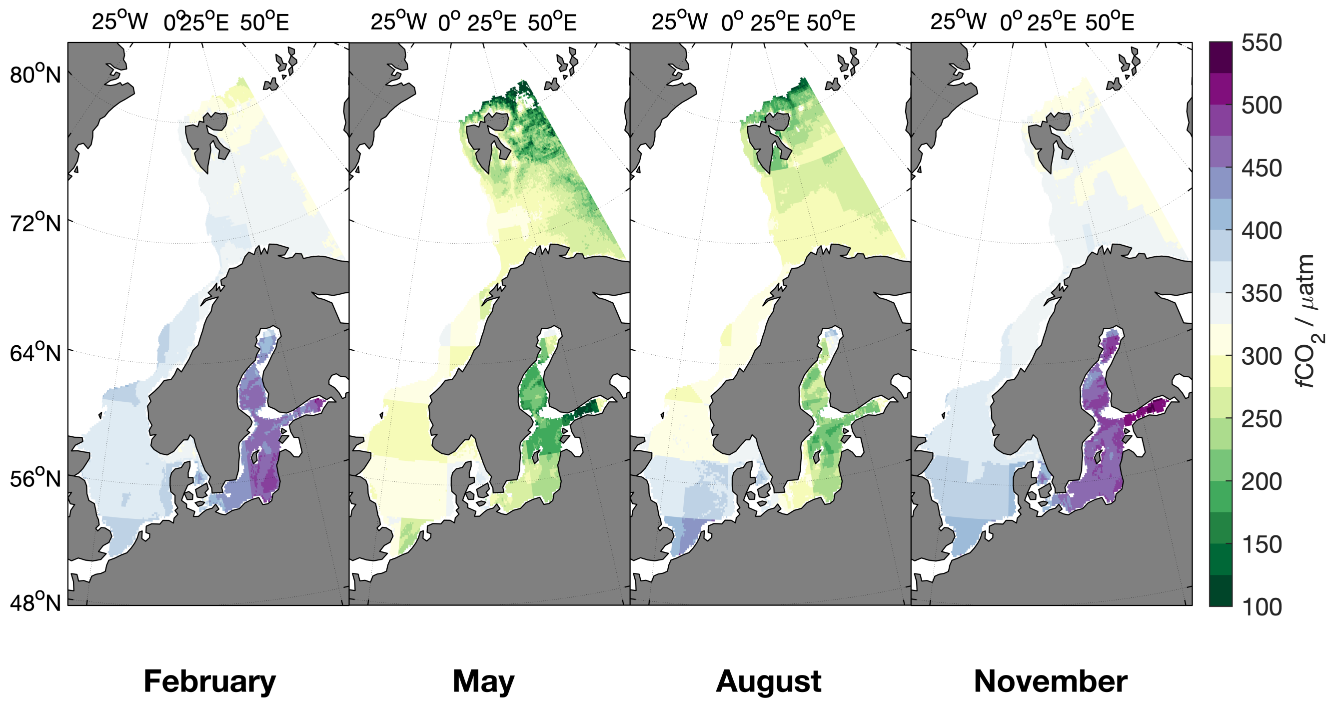

Figure 4. The average fCO_2 of MLR 1 (1998-2016) for one example months in each season (February, May, August and November).

3.2 Maps of pH

The monthly average of pH calculated from MLR 1 fCO_2 is ranging from about 8 during winter to 8.15 during summer in the North Sea and at the Norwegian coast (Figure 5). Towards the Barents Sea the pH maximum increases during summer to 8.2. The pH of 8.00 - 8.15 in regions with a large influence from the Atlantic, such as the northern North Sea and the Norwegian coast, is in good agreement with the range of pH determined for the open North Atlantic (Lauvset and Gruber, 2014; Lauvset et al., 2015). In the North Sea, the pH is in the same range as reported in Salt et al. (2013) and it also shows the same distribution in August/September with higher pH in the northern North Sea and lower pH in the southern part.

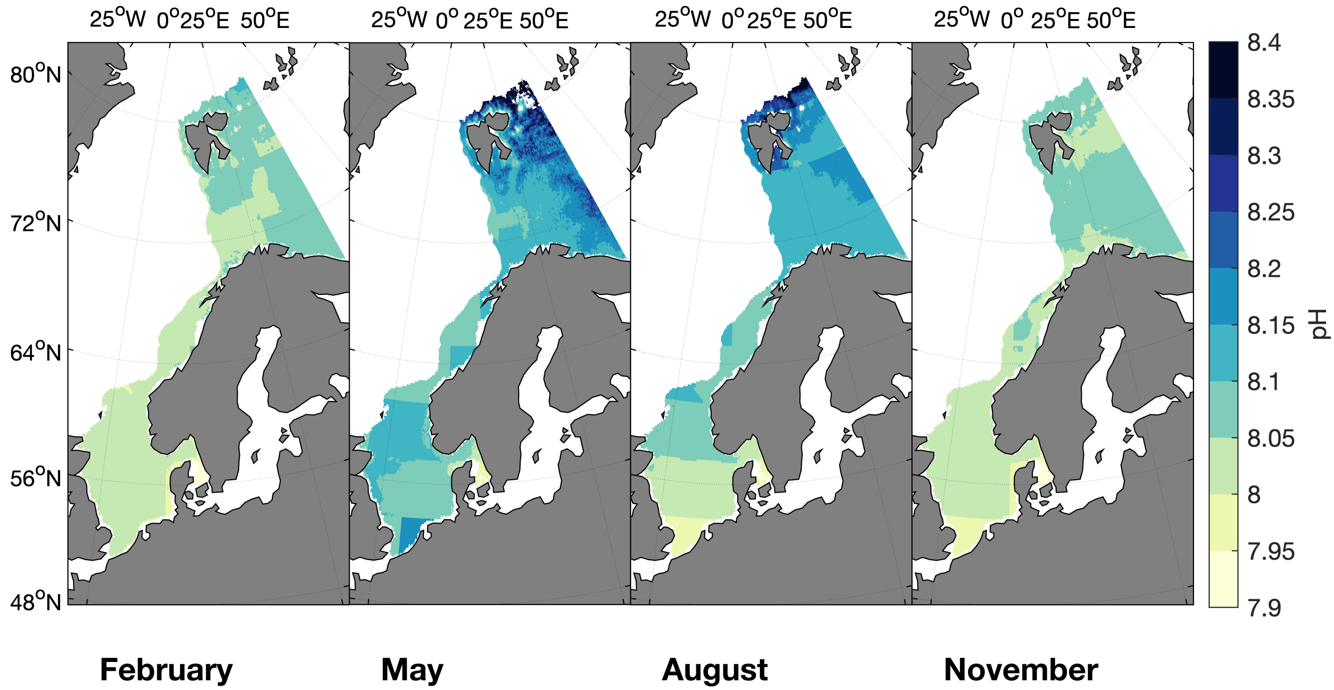

Figure 5. The average pH based on MLR 1 (1998-2016) for one example month in each season (February, May, August and November).

4 Discussion

4.1 ~~Validation~~ Performance of the pCO_2 maps

The performance of the MLR and the produced maps are evaluated in different ways: (1) the R^2 and the RMSE of the fit between the driver data and the gridded observations, (2) the average deviation and its standard deviation, as well as the ME between the produced fCO_2 maps and the gridded observations as a regional average, (3) showing the median deviation between the MLR and the gridded observations on a monthly level, (4) by comparing the data from the fCO_2 maps to observations from two time series stations. (2) - (4) will be shown for both, the time period covered by the driver data (1998-2016) and a prediction of the maps into the years 2017 and 2018. The prediction of the maps into the years 2017 and 2018 will be compared with data from the newest SOCAT release (SOCATv2019) to have a comparison with an independent dataset. Please note that the comparability of the model performance between the different regions is limited. All used statistical parameters are influenced by characteristics that can vary substantially between the different regions, such as range of the data, their variability or the amount of grid cells with data. Additionally, in a region with many measurements the amount of variability captured by these measurements is most likely larger and, thus will lead to a weaker correlation.

Generally, the uncertainty of MLR 1 are in the same range as in other studies (Laruelle et al., 2017; Yasunaka et al., 2018) mapping coastal fCO_2 dynamics: 25 μatm in the North Sea, 16 μatm along the Norwegian Coast, 12 μatm in the Barents Sea, and 39 μatm in the Baltic Sea (based on the RMSE in Table 5). In the Baltic Sea, which has a large variability in itself, Parard et al. (2016) obtained lower standard deviations through dividing the area in smaller sub-regions.

The seasonal differences between MLR 1 and the SOCAT v5 data for each region are shown in Figure 6. This comparison shows a very good agreement. For MLR 1, the seasonal variations of the median bias are small in the North Sea, along the Norwegian coast and in the Baltic Sea. In the Barents Sea, however, the bias varies seasonally. Here, MLR 1 slightly underestimates the fCO_2 in winter and early spring, while it overestimates the fCO_2 in summer. In all other regions, the median seasonal bias is smaller than the uncertainty of the maps. The larger seasonal bias in the Barents sea is most likely caused by the larger seasonal bias in the number of available observations. There is no data available in October, December and January.

When comparing all observations from the years 2017 and 2018 to the predictions by the ~~MLR1~~MLR 1, we find a good agreement in the North Sea (2 ± 20 μatm) and no seasonal bias (Figure 7). In the other regions, the agreement is somewhat reduced compared to the years 1998-2016 (-9 ± 39 μatm (Norwegian Coast), -5 ± 29 μatm (Barents Sea) and 28 ± 58 μatm (Baltic Sea)). In these regions we also observe a seasonal bias in the years 2017 and 2018. At least for the Baltic Sea this could be a ~~reason of a~~ result of the extraordinarily warm and dry summer in 2018, that lead to very low fCO_2 values in the Baltic Sea ~~Bakker et al. (2016) Please note~~(see Figure 8 and the data in SOCAT Bakker et al. (2016)). Please note, that for this comparison ~~,~~ the MLR was extrapolated in time. Only observations until December 2016 were used to produce the MLR. Therefore accuracy of the maps itself is reduced.

In a second test to investigate to which extent MLR 1 can reproduce observations we compared the MLR output with time series data from two voluntary observing ship lines in two very different regions with a good data coverage: M/V Nuka Arctica in the northern North Sea (0-2°E, 58-60°N) and M/V Finnmaid in the Baltic Sea (23-24°E, 59-60°N) (Figure 8). To every observation we assigned the related value of MLR 1. The agreement between the MLR 1 and the observations is very good. MLR 1 reproduces the general seasonality and some of the interannual variability, also in the years 2017 and 2018, of which the observations were not used in the regression.

When performing interpolation exercises it is always important to be aware of the fact that the resulting maps might come with biases and do not represent all regions equally well. While the here presented maps give a good general overview about the surface ocean fCO_2 variability in regions with a relatively large amount of data, the reliability, however, is limited in those regions where the data coverage is more scarce. This is especially the case, when the region with scarce data coverage is showing different characteristics in, for example, temperature and salinity, compared to the rest of the region. One such example is the Gulf of Bothnia in the Baltic Sea region where almost all data used to derive the MLR is from south of 60°N i.e. not in the Gulf of Bothnia, but in the Baltic Proper and western Baltic Sea (Figure 2). The MLR method can also lead to unrealistic extreme values and even negative fCO_2. Some such values occur in the northeastern Barents sea as well as in

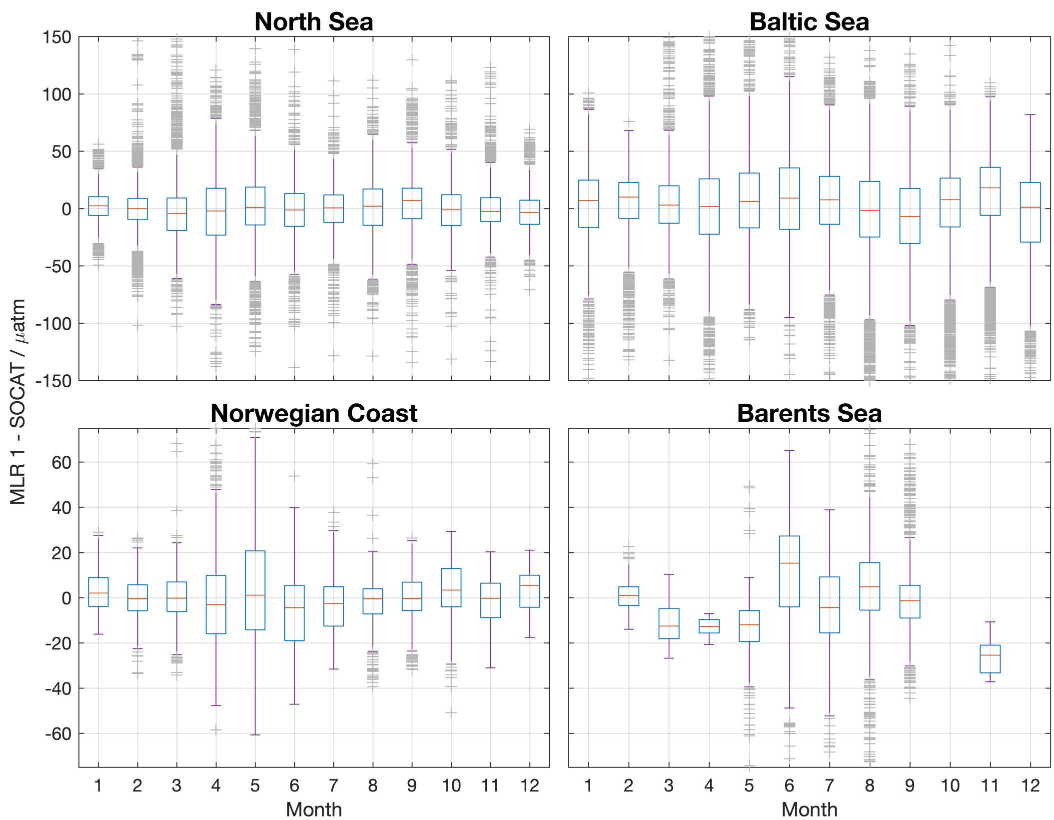

Figure 6. Boxplots showing the median deviation of MLR 1 from the gridded SOCAT v5 5 data for each region (red line). The boxes show the respective 75% percentiles. 99% of the data lays within the range of the purple whiskers. Extremes are shown as gray crosses.

some parts of the Baltic Sea (about 0.01% of the grid cells in each region). As pH cannot be calculated for negative $f\mathrm{CO_2}$, we excluded all negative $f\mathrm{CO_2}$ values for the calculation of pH. Excluding the negative values resulted in a change of the average $f\mathrm{CO_2}$ of 0.05 μatm (Baltic Sea) and 0.3 μatm (Barents Sea) so they are of negligible importance for the flux estimates. While the negative values are easy to spot and discard there are most likely more unrealistically low values in spring and summer data in the very north and northeastern Barents Sea as well as some parts of the Baltic Sea. However, there are no data available in SOCAT v5 or elsewhere available to validate thisto validate this.

All regions with questionable $f\mathrm{CO_2}$ are also questionable in their pH data. There is a number of very high pH in the Barents Sea, that are associated with also very low $f\mathrm{CO_2}$ that might not be realistic. In addition, estimated pH values in regions or seasons low salinity regions where the actual alkalinity-salinity deviates strongly from the Nondal et al. (2009) one used here (e.g. river mouths in the southern North Sea or the Skagerrak), should be interpreted with caution.

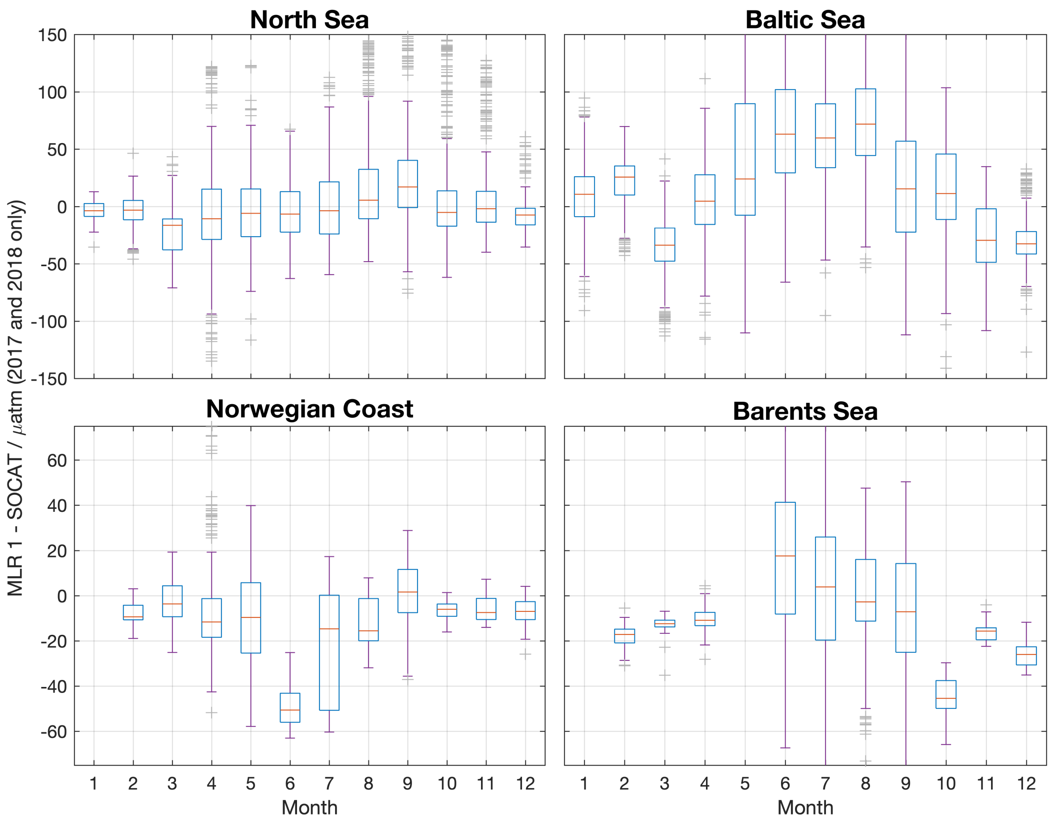

Figure 7. Boxplots showing the median deviation of MLR 1 (based on observations until 2016) predicted and measured fCO_2 values in 2017 and 2018. The boxes show the respective 75% percentiles. 99% of the data lays within the range of the purple whiskers. Extremes are shown as gray crosses. The number of grid cells with data available were: North Sea: 5047 , Norwegian Coast: 1543, Barents Sea: 2312, Baltic Sea: 5414.

4.2 Trends in fCO_2 and pH

The trends in surface ocean fCO_2 in coastal regions are often difficult to assess because of the scarcity of the data relative to the highly dynamical character of these regimes and their large interannual variability. One issue is that the start of the productive season can range from February to April even within a small area, such that even restricting the analysis to specific seasons (e.g. winter) can be challenging. However, due to lack of data, especially winter data, most observational studies are based on repeated sections during summer. Further, the fact that these measurements typically do not take place every year, adds even more uncertainty to the estimated trend, as the interannual variability can mask the trend signal.

The monthly maps of fCO_2 from 1998 to 2016 enable us now to estimate the trend in surface ocean fCO_2 for the entire region~~and~~, equally distributed over the seasons (Figure 9, left). All trends were computed by using deseasonalized data. The interannual variability of the trend estimates in each region is shown in the panels on the right hand side in Figure 9. Based

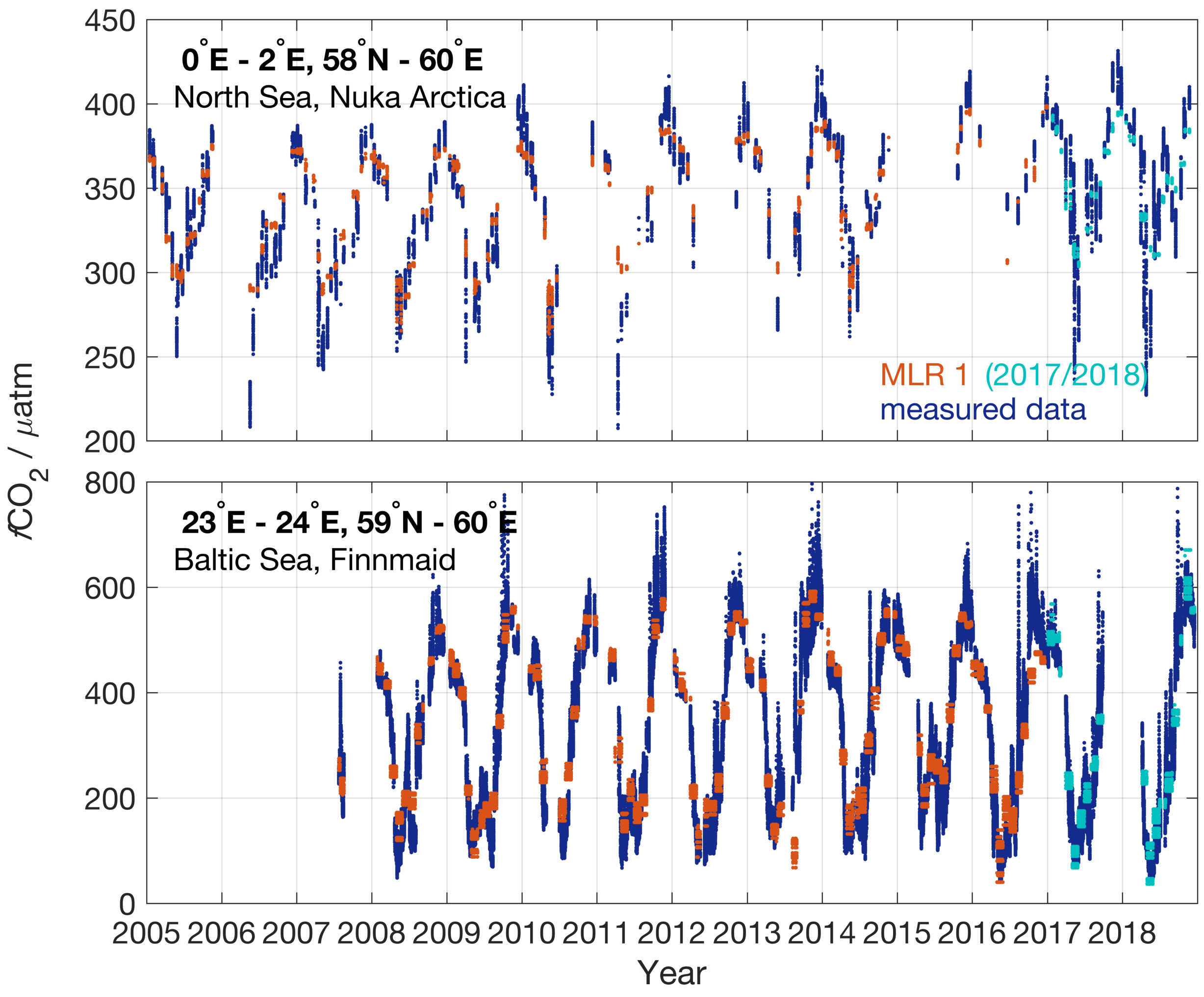

Figure 8. Time series of VOS data from Nuka Arctica (upper panel, blue) and Finnmaid (lower panel, blue) compared with MLR 1 at the same location (red). In light blue the predictive MLR output for the years 2017 and 2018 is shown.

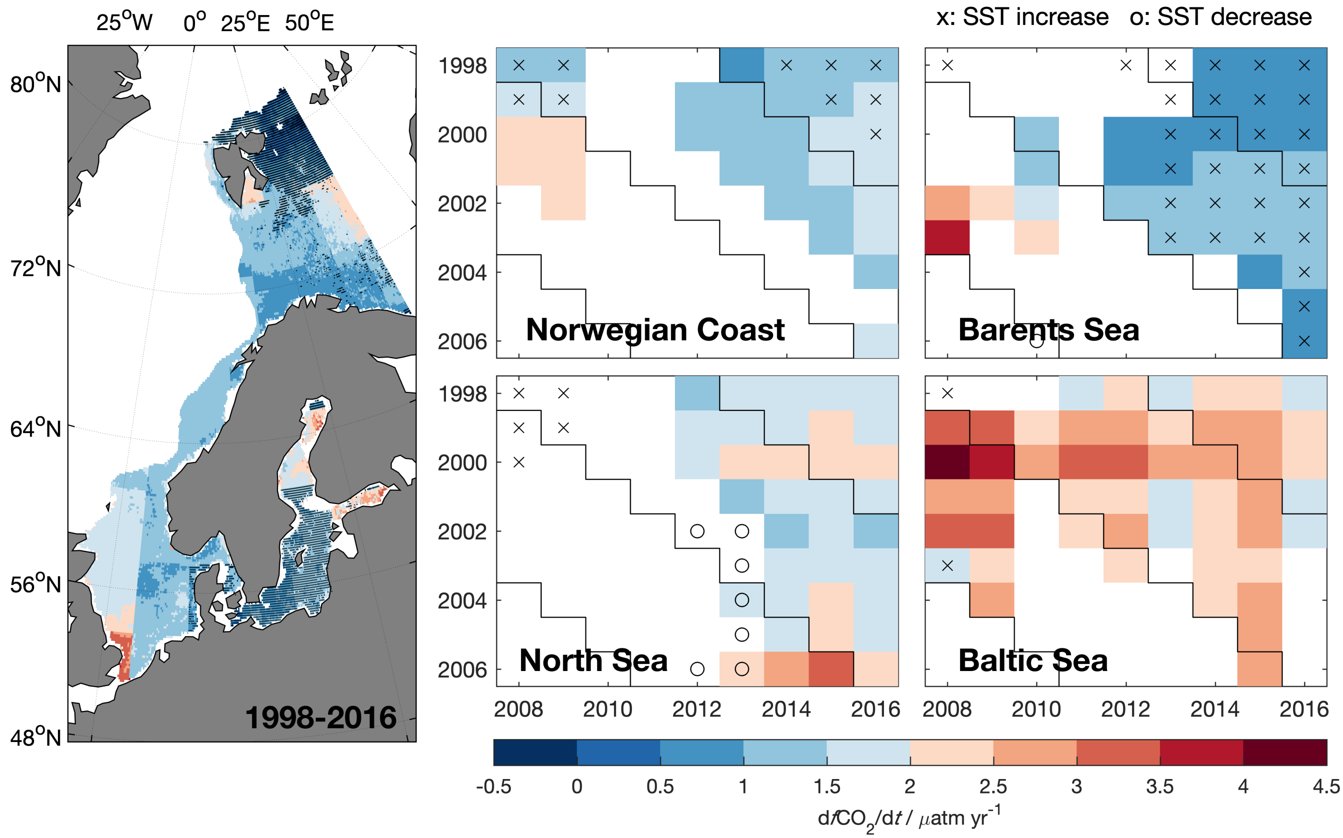

Figure 9. The trend in surface ocean $f\text{CO}_2$ estimated from deseasonalized $f\text{CO}_2$. The left hand panel show the spatial distribution of the trend over the time period from 1998 to 2016. Grid boxes without a significant trend are denoted with a black dot. On the right hand the influence of the time range on the average trend is shown for the four regions. Non significant trends were left blank. Significant trends in sea surface temperature are indicated with crosses/circles.

on the linear regression the significant trends in $f\text{CO}_2$ have an average uncertainty of 0.5 μatm/yr (North Sea), 0.4 μatm/yr (Norwegian Coast), 0.4 μatm/yr (Barents Sea), and 0.7 μatm/yr (Baltic Sea), while the shorter time periods shown have a higher and the longer time periods a lower uncertainty. For pH trends the average uncertainty of the regression is $5 \cdot 10^{-4}$ (North Sea) and $7 \cdot 10^{-4}$ (Norwegian Coast and Barents Sea).

~~The trend in surface ocean pH estimated from deseasonalized pH. On the left hand the spatial distribution of the trend over the time period from 1998 to 2016 is shown. Grid boxes without a significant trend are denoted with a black dot. On the right hand the influence of the time range on the average trend is shown for the four regions. Non significant trends were left blank.~~

In most of the regions addressed in this study, the trend in the surface ocean is lower than the trend in atmospheric $x\text{CO}_2$ (global average 2.02 ppm yr $^{-1}$ ("Cooperative Global Atmospheric Data Integration Project", 2015)). Trends exceeding the

Table 6. fCO_2 trend calculated from gridded, deseasonalized SOCAT v5 observations.

Region	Latitude / °N	Trend / μatm yr^{-1}
North Sea, South	51 - 54.5	3.2 ± 1.3
North Sea, Center	54.5 - 58	1.43 ± 0.21
North Sea, North	58 - 62	2.320 ± 0.089
Norwegian Coast, South	62 - 68	2.12 ± 0.19
Norwegian Coast, North	68 - 73	1.426 ± 0.099
Barents Sea, South	69 - 74	1.31 ± 0.30
Barents Sea, North	74 - 85	1.01 ± 0.22
Baltic Sea, South	54 - 56	2.05 ± 0.12
Baltic Sea, North	56 - 61	1.84 ± 0.21

atmospheric values in the period from 1998 to 2016 can only be observed at the entrance of the English Channel, in Storfjorden/Svalbard, the Gulf of Finland and the Gulf of Bothnia ($2.5-3$ μatm yr^{-1}). It has to be noted that there was almost no measured fCO_2 as MLR input in neither Storfjorden nor the Gulf of Bothnia. Therefore, these trends should be handled with care. The western North Sea has a trend that is only slightly lower than the trend in the atmosphere ($1.5-2$ μatm yr^{-1}), while the trends in the eastern North Sea, along the Norwegian coast and in the Barents Sea are somewhat lower (0.5-1.5 μatm yr^{-1}). In the North Sea this is consistent with a recent study directly based on observations Omar et al. (2019). ~~The low trends~~ These low trends will result in an increase in the strength of the ocean carbon sink with time. ~~A trend smaller than the atmospheric trend can be caused by a shift in the bloom onset. For example, in the North Seaa significant drawdown in~~

The northern European shelf is a region with a high data density. In order to validate the general patterns of fCO_2 ~~has been observed as early as February in some years (Omar et al., 2019). The bloom onset in the North Sea after the 1990s has been shown to be mainly triggered by the spring-neap tidal cycle and the air temperature by Sharples et al. (2006). They found that the onset of spring bloom has occurred on average 1 day earlier every year. Over the period covered in this study (almost 20 years)this could cause a change of three weeks in the timing of the spring bloom. Even if the trend in winter~~ trends we estimated the fCO_2 ~~was following the atmospheric xCO_2 increase, such a change in bloom onset would lead to a trend lower than the atmospheric when averaging over the entire year.~~ trends also from the SOCAT v5 observations, that were used to produce the MLR (Table 6). We gridded and deseasonalized the SOCAT v5 data and divided the entire region into 9 subregions. A figure showing the fits and the data coverage can be found in Appendix A. These observation based trends show similar general patterns as those based on our maps (Figure 9, 1998-2016): (1) largest trends in the southern North Sea, (2) decreasing towards the North with trends around the atmospheric trend in the northern North Sea and trends around 1 μatm yr^{-1} in the Barents Sea, (3) close to atmospheric trends in the Baltic Sea.

The observation that large subareas (the Baltic Sea , the or along the shore of the western North Sea) did not show a significant trend can be explained by the factthat, coastal , that coastal sea systems, especially enclosed areas as the Baltic Sea, experience a high anthropogenic pressure. Anthropogenic impacts other than rising atmospheric CO_2 concentrations influencing the ocean carbon system and the bloom properties such as the nutrient load of rivers can effect coastal ecosystems through eutrification, resulting eutrophication. This will result in lower $f CO_2$ in summer and higher $f CO_2$ in winter (Borges and Gypens, 2010; Cai et al., 2011). Another important process that influences the carbon system in the Baltic Sea are inflow events from the North sea. In between such events, CO_2 accumulates in deeper water layers causing an increasing gradient of dissolved inorganic carbon (DIC) across the halocline. Whenever deep winter mixing occurs, this will then lead to a large increase of surface $f CO_2$ because of the input of DIC rich waters from below. Another reason is the observed change in alkalinity with time which effects the $f CO_2$ though changes in the buffer capacity of the inorganic carbon system (Müller et al., 2016).

One reason for a trend smaller than in the atmosphere can be a shift in the bloom onset. For example, in the North Sea a significant drawdown in $f CO_2$ has been observed as early as February in some years, but there is also a large variability (Omar et al., 2019). The bloom timing and onset in the North Sea after the 1990s has been shown to be mainly triggered by the spring-neap tidal cycle and the air temperature (Sharples et al., 2006). The bloom timing and onset was found to be significantly earlier in the 2010s compared to the previous decades (Desmit et al., 2020). Even if the trend in winter $f CO_2$ was following the atmospheric $x CO_2$ increase, such a change in bloom timing and onset would lead to a trend lower than the atmospheric when averaging over the entire year. The hypothesis, that an earlier or more intense bloom onset is responsible for the relatively low trends in the North Sea is supported by looking at the contributions of the different months to the overall trend. Figure 10 shows the trend for each month in the four different regions.

When looking at the interannual variability, it becomes obvious that the trend in the North Sea is slightly smaller than the atmospheric CO_2 trend. In contrast, the Norwegian coast and the Barents Sea experience a robust trend much lower than the atmospheric trend (Norwegian Coast: $1 - 1.5$ μatm yr^{-1}, Barents Sea: around 1 μatm yr^{-1}). Here we can also see a stable pattern of warming over time scales of 10 to 15 years. The warming in itself would result in an increase of $f CO_2$ with time, in addition to the atmospheric forcing. As we are observing a trend smaller than the atmospheric trend, temperature effects can't be the driver here. The lower trend stems most likely from an earlier onset of spring bloom. It has been shown that the atlantification and the reduced ice coverage of the Barents sea leads to a longer productive season, and this will result in more months with strong undersaturation in CO_2 (Oziel et al., 2016). In the Baltic Sea the pattens are different. Here the variability is much larger, while most of the time periods show a trend larger than the atmospheric trend ($3 - 3.5$ μatm yr^{-1}). Although slightly smaller our results broadly agree with trend estimates based on measurements of 4.6 - 6.1 μatm yr^{-1} over 2008-2015 (Schneider and Müller, 2018). Finally, it also needs to be noted that the uncertainty of the $f CO_2$ maps was highest in the Baltic Sea. This makes it also more difficult, if not impossible, to properly detect these small trends.

For pH, the trend in most regions is around -0.002 yr^{-1} (Figure 11). A expected, regions with the strongest trend in $f CO_2$ also show the highest trend in pH, such as the southern North Sea. The trend in the northern North Sea and along the Norwegian

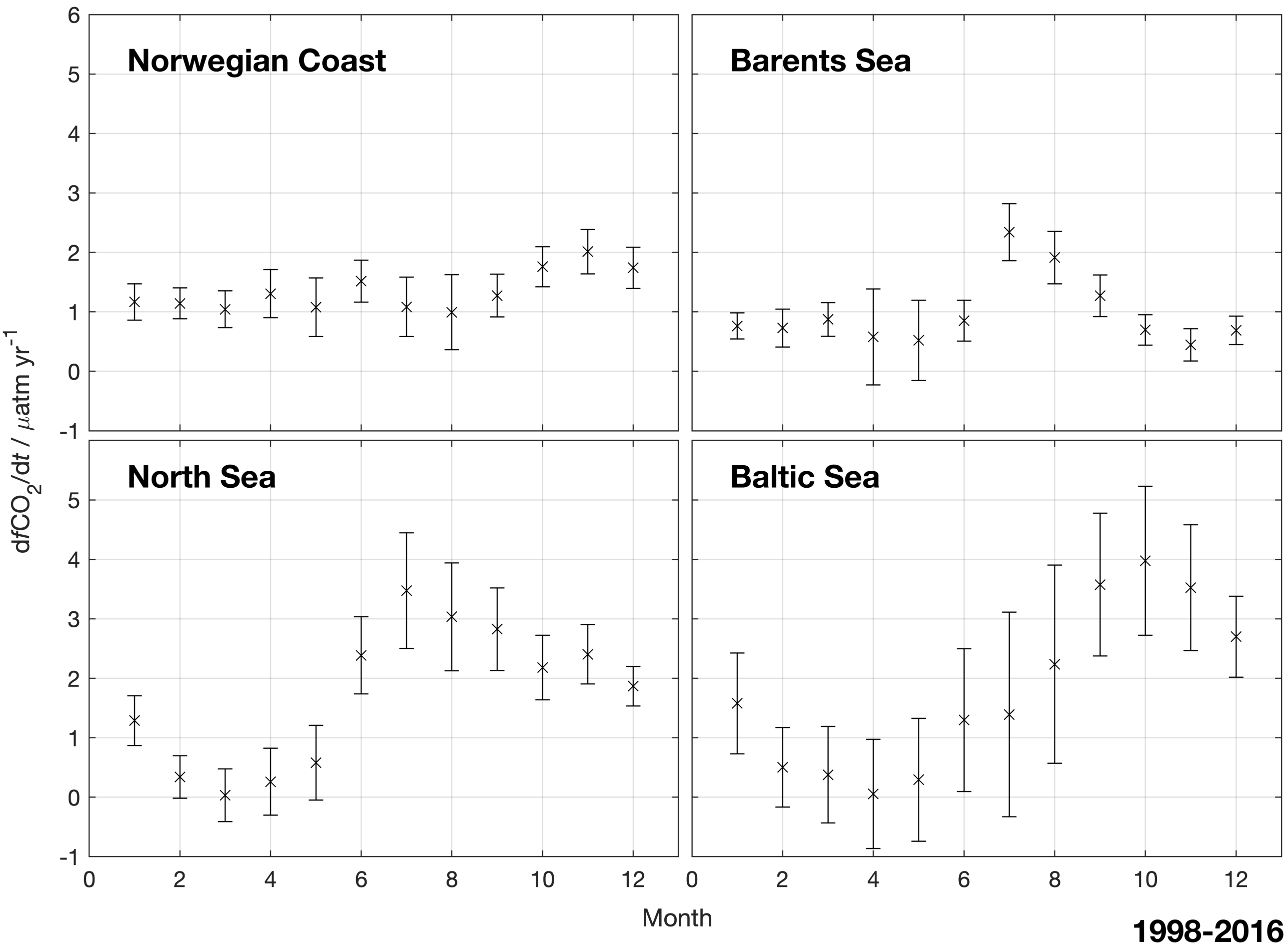

Figure 10. The trend in surface ocean fCO_2 estimated resolved per month (1998 to 2016).

Coast is in good agreement with the pH trends found in studies focusing on the open Atlantic Ocean (-0.0022 yr^{-1} (Lauvset and Gruber, 2014)) and the North Atlantic and Nordic Seas (-0.002 yr^{-1} (Lauvset et al., 2015)).

4.3 CO_2 disequilibrium and flux

The average sea-air CO_2 disequilibrium (ΔfCO_2=$fCO_{2,\mathrm{sea}} - fCO_{2,\mathrm{atm}}$) is shown in Figure 12. The only region showing an average supersaturation is the southern North Sea. Towards the north, the surface ocean becomes more and more undersaturated, with lowest values in the Barents Sea. The values we found in the Barents Sea (-60 to -80 μatm in the southern Barents Sea and less than -100 μatm around Svalbard) are in generally in agreement those estimated by Yasunaka et al. (2018). The seasonal cycle of ΔfCO_2 follows a mainly biologically driven pattern with higher values in the winter and lower values from April to August. The seasonal cycle is largest in the Baltic and smallest in the Barents Sea.

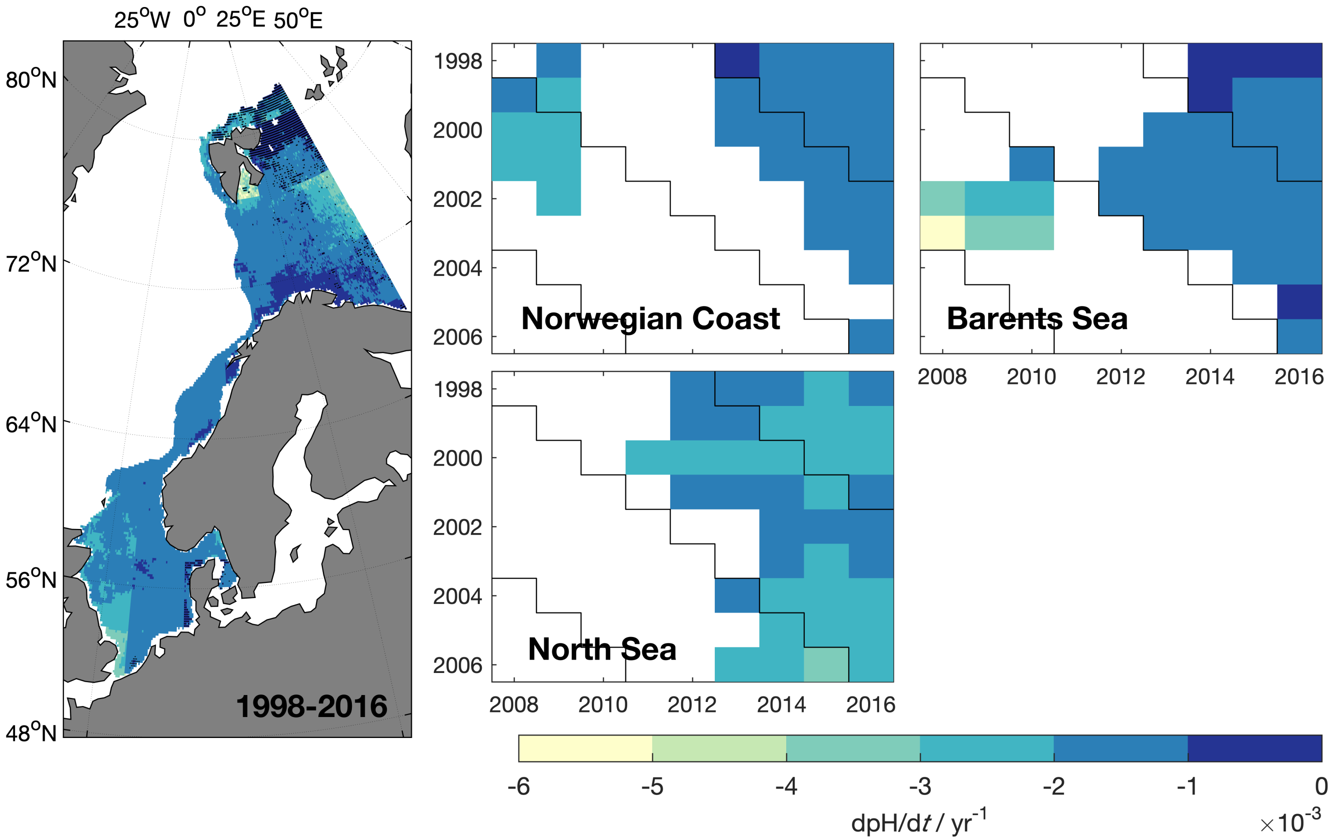

Figure 11. The trend in surface ocean pH estimated from deseasonalized pH. On the left hand the spatial distribution of the trend over the time period from 1998 to 2016 is shown. Grid boxes without a significant trend are denoted with a black dot. On the right hand the influence of the time range on the average trend is shown for the four regions. Non significant trends were left blank.

The sea-air CO_2 fluxes (Figure 13) show that most regions are a net and increasing sink for CO_2. The only source net regions are the southern North Sea and the Baltic Sea. The two different regimes in the North Sea with the southern, non-stratified part being a source and the northern temporarily stratified part a sink for CO_2, are well have been described in the literature (Thomas et al., 2004). before (Thomas et al., 2004). However, there is a large interannual variability in the fCO_2 disequilibrium (Omar et al., 2010). This is reflected in the fact that studies based on different years find conflicting results regarding the direction of the flux (Schiettecatte et al., 2007; Thomas et al., 2004). This large interannual variability can also be found in our maps. During some years larger parts of the North Sea were a net source, while during other years also the southern North Sea acted as net sink.

The seasonal variations in the air-sea flux are driven by a combination of the changes in the disequilibrium, the wind strength, and the ice cover. As there is less wind during summer, when the disequilibrium is large, but a smaller disequilibrium during

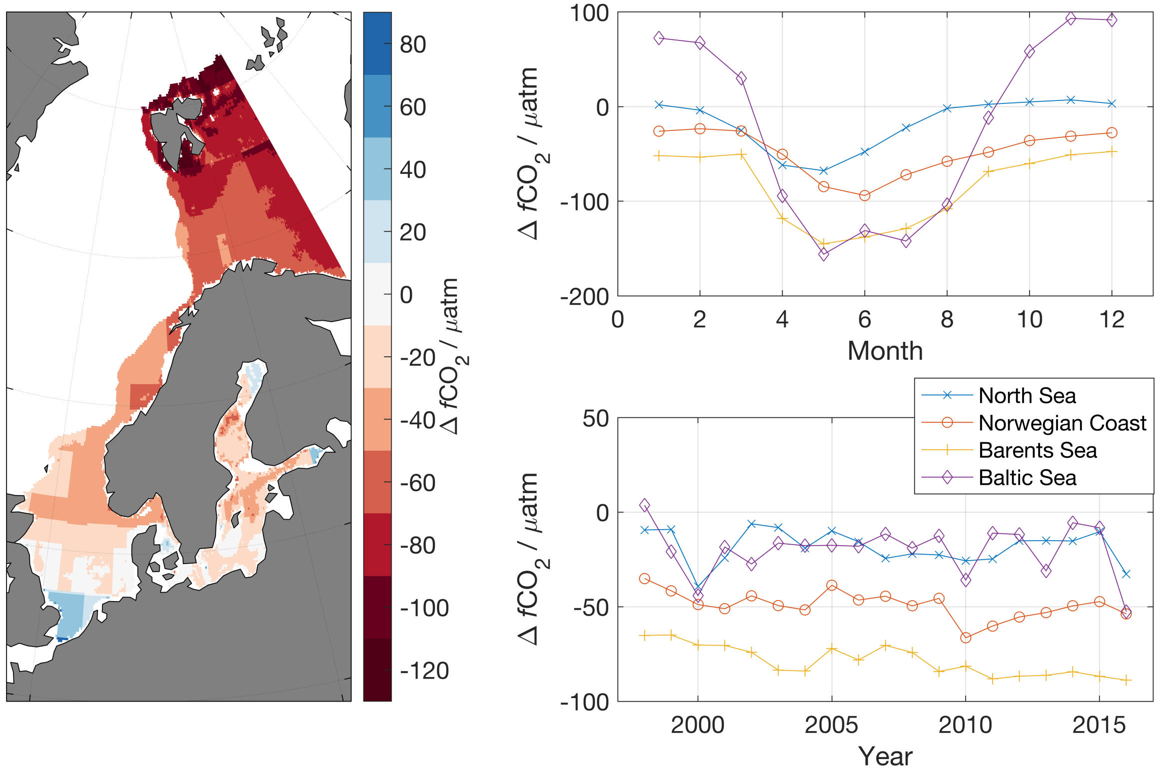

Figure 12. The average air-sea CO_2 disequilibrium over the period 1998-2016 (left hand panel, red colors indicate average undersaturation, while blue colors indicate average oversaturation). For every region average disequilibria are shown as seasonal averages (right side, upper corner) and time-series of annual disequilibria (right side, lower corner). Blue line: North Sea, red line: Norwegian coast, yellow line: Barents Sea, purple line: Baltic Sea

winter, when the wind strength is high, the seasonal variability is often less clear than that of e.g. the disequilibrium. This can be seen in the Barents Sea and Norwegian Coast. Yasunaka et al. (2018) found the seasonal and interannual variation in the Barents Sea and the Norwegian Sea mostly corresponded to the wind speed and the sea ice concentration. In contrast to that we see the strongest dependence on the air-sea disequilibrium. However, even though we don't find the same seasonality, considering the error margin and the small amplitude of the seasonality, our average fluxes fit well with those reported by Yasunaka et al. (2018) of -8 to -12 mmol m^{-2} d^{-1} (Barents Sea) and -4 to -8 mmol m^{-2} d^{-1} (Norwegian Coast). In the North Sea there is almost no net flux during winter, as the surface ocean is more or less in equilibrium with the atmosphere. In the Baltic Sea, we can see high fluxes into the atmosphere during winter as here a large oversaturation coincides with high wind strengths. This is also why the Baltic Sea is a net source regions. Although Parard et al. (2017) did find slightly smaller fluxes (+15 mmol m^{-2} d^{-1} during winter and -8 mmol m^{-2} d^{-1} during summer), the annual air-sea CO_2 fluxes are in good agreement (0 to +4 mmol m^{-2} d^{-1} between 1998 and 2011).

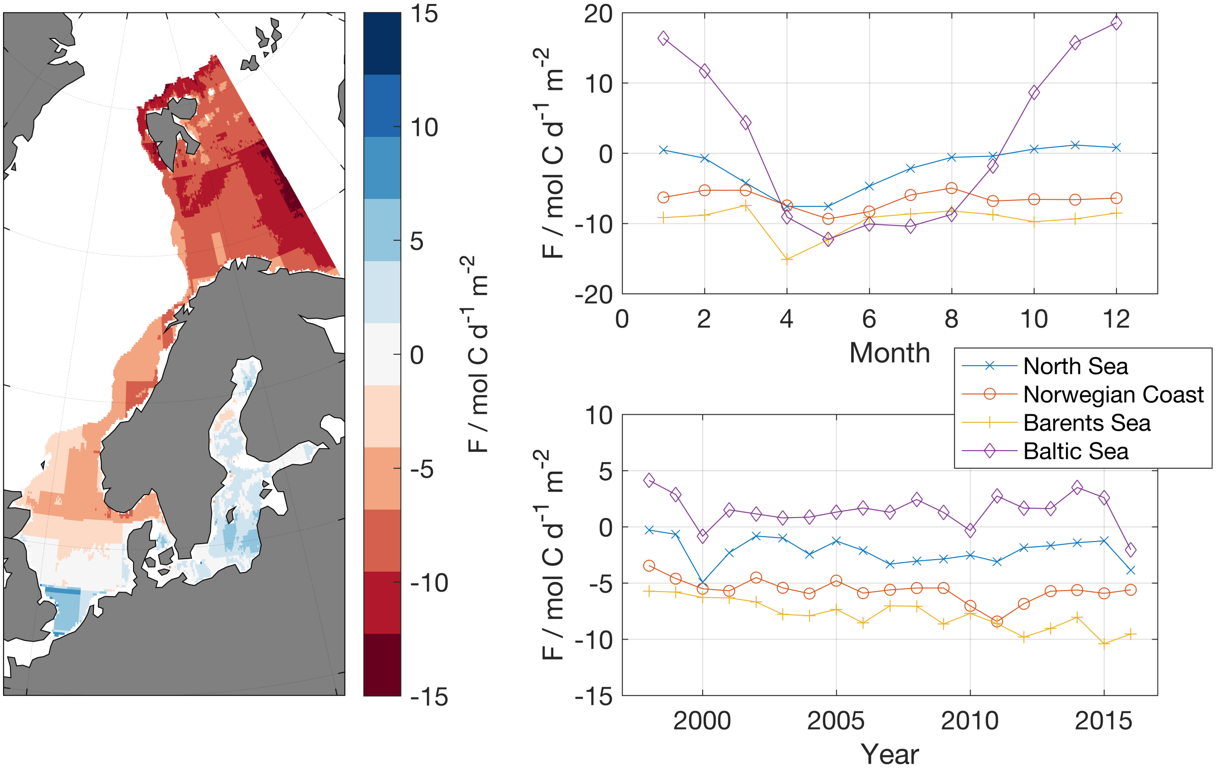

Figure 13. The average air-sea CO_2 flux over the period 1998-2016 (left hand panel, red colors indicate sink regions, while blue colors indicate source regions). For every region average fluxes are show as seasonal averages (right side, upper corner) and timeseries of annual fluxes (right side, lower corner).

The uncertainty in the calculated fluxes is a result of the uncertainties in the fCO_2 observations, ΔfCO_2 maps, the gas exchange parameterization and the wind product. The uncertainty of the ΔfCO_2 is mostly driven by the uncertainty of the MLR, resulting in an error between 12 μatm and 39μatm, according to the RMSE values of MLR1 for the different regions (Table 5). A number of studies addresses on the uncertainty of gas exchange parameterizations and the wind products (Couldrey et al., 2016; Gregg et al., 2014; Ho and Wanninkhof, 2016). For this study, we apply an uncertainty of the gas transfer velocity of 20% (Wanninkhof, 2014). This will result in an uncertainty of the air-sea flux of about 2 mmol C d^{-1} m^{-2}. It has to be kept in mind, that the absolute uncertainty in k increases with increasing wind speed, but that the uncertainty in the wind speed has largest influence in summer when also the disequilibrium is large. In contrast to that the uncertainty in ΔfCO_2 will cause larger errors in winter, when the wind speeds are high.

5 Conclusions

The MLR approach presented in this work is a relatively easy and straight forward method to produce monthly fCO_2 maps with a high spatial resolution in coastal ~~regions~~seas. Using available open ocean maps did improve the coastal maps significantly. The maps reproduce nicely the main spatial and temporal patterns that can also be found in observations in the different regions for both fCO_2 and pH. The surface seawater fCO_2 trends were mostly lower than the atmospheric trends and also lower than the trends found in the open North Atlantic. We did find the northern European shelf to be an increasing net sink for CO_2. Only the Baltic Sea is a net source region. This method clearly has the potential to be extended to a larger region. However, it should be handled with care in regions with only a small number of observations as the MLR can lead to unrealistic values.

Longterm observations with a high temporal resolution are extremely important for developing maps such as presented here. While a decent spatial coverage exists for the open North Atlantic, most coastal regions are still undersampled. This is in particular the case for higher latitudes and in the Arctic. To further understand and interpret the trends on fCO_2 and pH it is necessary to increase our knowledge and understanding of the interaction of primary production, respiration in the water column and the sediments, mixing and gas exchange and their influence on the carbon cycle.

While MLR derived sea surface provides coherent picture of the entire region, they have clear limitations and should be interpreted with caution in regions with few or none observations. Both, for producing high quality maps, as well for their validation a large number of observations is essential.Also, observations of second parameter of the carbon system would be beneficial for deriving pH maps. This will help to reduce and quantify the error introduced by estimating alkalinity from salinity. In addition to that, our work neglects the areas closest to land due to unavailability of CO_2 data and reanalysis products in those areas. For adding their contribution to the flux estimates, new platforms specialized on measurements directly at the land-ocean interface need to be developed.

Data availability. The dataset is available under: https://doi.org/10.18160/939X-PMHU.

Appendix A: Trend in surface ocean fCO_2 observations

Competing interests. The authors declare no competing interests.

Acknowledgements. First of all, we want to thank everyone involved in the collection and quality control of surface ocean CO_2 data. The Surface Ocean CO_2 Atlas (SOCAT) is an international effort, endorsed by the International Ocean Carbon Coordination Project (IOCCP), the Surface Ocean Lower Atmosphere Study (SOLAS) and the Integrated Marine Biosphere Research (IMBeR) program, to deliver a uniformly quality-controlled surface ocean CO_2 database. The many researchers and funding agencies responsible for the collection of data and quality

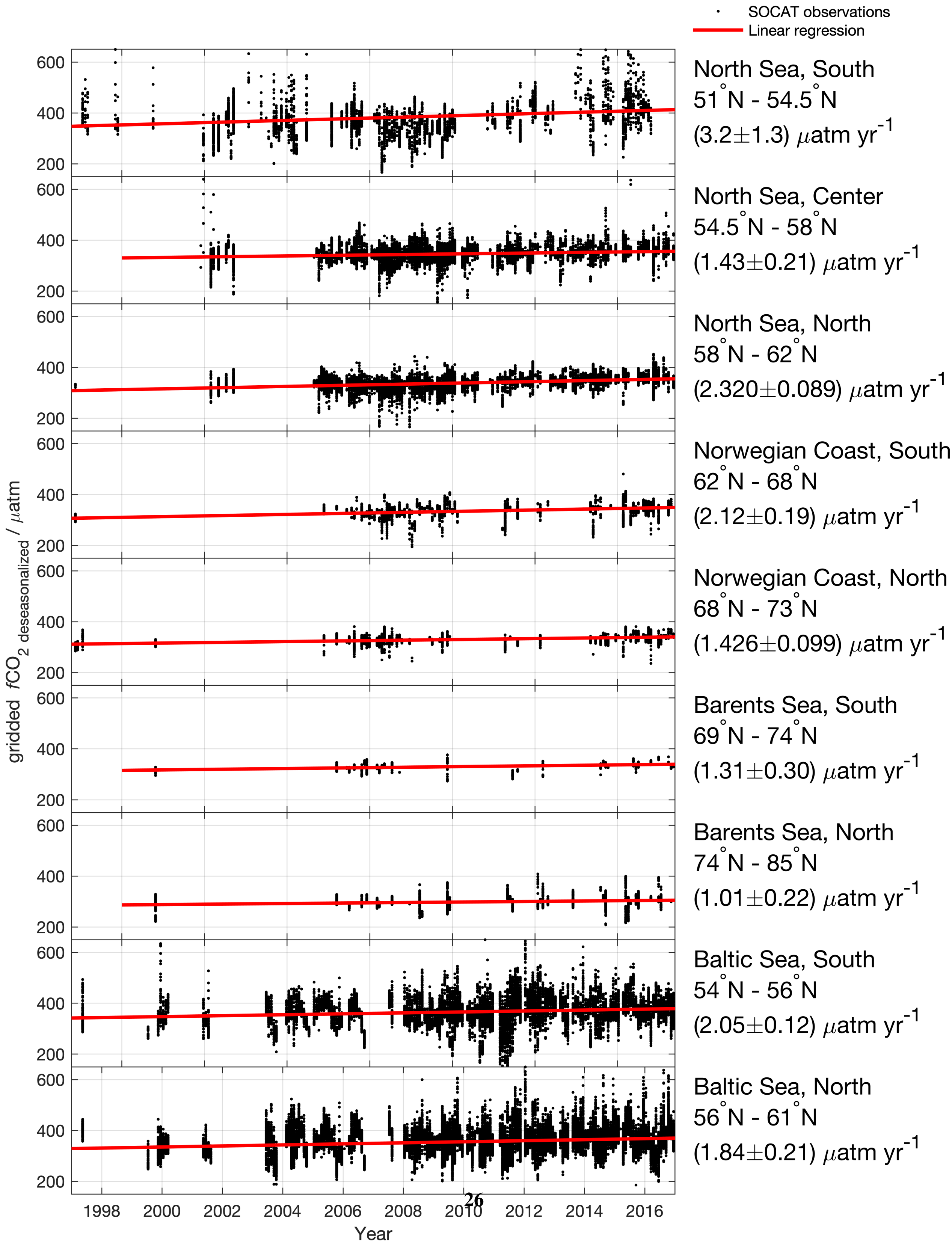

SOCAT observations
Linear regression
North Sea, South
51°N - 54.5°N
(3.2±1.3) μatm yr-1
North Sea, Center
54.5°N - 58°N
(1.43±0.21) μatm yr-1
North Sea, North
58°N - 62°N
(2.320±0.089) μatm yr-1
Norwegian Coast, South
62°N - 68°N
(2.12±0.19) μatm yr-1
Norwegian Coast, North
68°N - 73°N
(1.426±0.099) μatm yr-1
Barents Sea, South
69°N - 74°N
(1.31±0.30) μatm yr-1
Barents Sea, North
74°N - 85°N
(1.01±0.22) μatm yr-1
Baltic Sea, South
54°N - 56°N
(2.05±0.12) μatm yr-1
Baltic Sea, North
56°N - 61°N
(1.84±0.21) μatm yr-1
gridded fCO2 deseasonalized / μatm
Year

control are thanked for their contributions to SOCAT. We used NCEP Reanalysis 2 data provided by the NOAA/OAR/ESRL PSD, Boulder, Colorado, USA, from their web site at https://www.esrl.noaa.gov/psd/. This study has been conducted using E.U. Copernicus Marine Service Information. This ~~work~~ research was funded by the ~~project ICOS Norway (~~Research Council of Norway ~~,~~ projects ICOS-Norway (Grant 245927) ~~. This project has received funding from the~~ and Nansen Legacy (Grant 276730); the VERIFY project (European Union's Horizon 2020 research and innovation program ~~under~~ grant agreement No ~~776810. This work was supported by BONUS INTEGRAL, receiving funding from BONUS (Art 185)by the EU and the contributing national funding agencies, Grant No. 03F0773A of the German Ministry for Education and Research.~~ 776810); and BONUS Integral.

References

Bakker, D. C. E., Pfeil, B., Landa, C. S., Metzl, N., O'Brien, K. M., Olsen, A., Smith, K., Cosca, C., Harasawa, S., Jones, S. D., Nakaoka, S.-i., Nojiri, Y., Schuster, U., Steinhoff, T., Sweeney, C., Takahashi, T., Tilbrook, B., Wada, C., Wanninkhof, R., Alin, S. R., Balestrini, C. F., Barbero, L., Bates, N. R., Bianchi, A. A., Bonou, F., Boutin, J., Bozec, Y., Burger, E. F., Cai, W.-J., Castle, R. D., Chen, L., Chierici, M., Currie, K., Evans, W., Featherstone, C., Feely, R. A., Fransson, A., Goyet, C., Greenwood, N., Gregor, L., Hankin, S., Hardman-Mountford, N. J., Harlay, J., Hauck, J., Hoppema, M., Humphreys, M. P., Hunt, C. W., Huss, B., Ibánhez, J. S. P., Johannessen, T., Keeling, R., Kitidis, V., Körtzinger, A., Kozyr, A., Krasakopoulou, E., Kuwata, A., Landschützer, P., Lauvset, S. K., Lefèvre, N., Monaco, C. L., Manke, A., Mathis, J. T., Merlivat, L., Millero, F. J., Monteiro, P. M. S., Munro, D. R., Murata, A., Newberger, T., Omar, A. M., Ono, T., Paterson, K., Pearce, D., Pierrot, D., Robbins, L. L., Saito, S., Salisbury, J., Schlitzer, R., Schneider, B., Schweitzer, R., Sieger, R., Skjelvan, I., Sullivan, K. F., Sutherland, S. C., Sutton, A. J., Tadokoro, K., Telszewski, M., Tuma, M., Heuven, S. M. A. C. v., Vandemark, D., Ward, B., Watson, A. J., and Xu, S.: A multi-decade record of high-quality $f\mathrm{CO_2}$ data in version 3 of the Surface Ocean CO_2 Atlas (SOCAT), Earth System Science Data, 8, 383–413, https://doi.org/https://doi.org/10.5194/essd-8-383-2016, https://www.earth-syst-sci-data.net/8/383/2016/, 2016.

Bauer, J. E., Cai, W.-J., Raymond, P. A., Bianchi, T. S., Hopkinson, C. S., and Regnier, P. A. G.: The changing carbon cycle of the coastal ocean, Nature, 504, 61–70, https://doi.org/10.1038/nature12857, https://www.nature.com/articles/nature12857, 2013.

Blanton, J. O.: Circulation processes along oceanic margins in relation to material fluxes, in: Ocean Margin Processes in Global Change, pp. 145–63, Wiley, New York, 1991.

Borges, A. V. and Gypens, N.: Carbonate chemistry in the coastal zone responds more strongly to eutrophication than ocean acidification, Limnology and Oceanography, 55, 346–353, https://doi.org/10.4319/lo.2010.55.1.0346, https://aslopubs.onlinelibrary.wiley.com/doi/abs/10.4319/lo.2010.55.1.0346, _eprint: https://aslopubs.onlinelibrary.wiley.com/doi/pdf/10.4319/lo.2010.55.1.0346, 2010.

Bourgeois, T., Orr, J. C., Resplandy, L., Terhaar, J., Ethé, C., Gehlen, M., and Bopp, L.: Coastal-ocean uptake of anthropogenic carbon, Biogeosciences, 13, 4167–4185, https://doi.org/https://doi.org/10.5194/bg-13-4167-2016, https://www.biogeosciences.net/13/4167/2016/, 2016.

Bricheno, L. M., Wolf, J. M., and Brown, J. M.: Impacts of high resolution model downscaling in coastal regions, Continental Shelf Research, 87, 7–16, https://doi.org/10.1016/j.csr.2013.11.007, http://www.sciencedirect.com/science/article/pii/S0278434313003725, 2014.

Cai, W.-J., Hu, X., Huang, W.-J., Murrell, M. C., Lehrter, J. C., Lohrenz, S. E., Chou, W.-C., Zhai, W., Hollibaugh, J. T., Wang, Y., Zhao, P., Guo, X., Gundersen, K., Dai, M., and Gong, G.-C.: Acidification of subsurface coastal waters enhanced by eutrophication, Nature Geosci, 4, 766–770, https://doi.org/10.1038/ngeo1297, https://www.nature.com/articles/ngeo1297, number: 11 Publisher: Nature Publishing Group, 2011.

Cavalieri, D. J., Parkinson, C. L., Gloersen, P., and Zwally, H. J.: Sea Ice Concentrations from Nimbus-7 SMMR and DMSP SSM/I-SSMIS Passive Microwave Data, Version 1, Monthly, doi:https://doi.org/10.5067/8GQ8LZQVL0VL, 1996.

Center, N. G. D.: 2-minute Gridded Global Relief Data (ETOPO2) v2, NOAA, https://doi.org/doi:10.7289/V5J1012Q, 2006.

"Cooperative Global Atmospheric Data Integration Project": Multi-laboratory compilation of atmospheric carbon dioxide data for the period 1968-2014, obspack_co2_1_GLOBALVIEWplus_v1.0_2015-07-30, https://doi.org/10.15138/G3RP42, published: NOAA Earth System Research Laboratory, Global Monitoring Division, 2015.

Couldrey, M. P., Oliver, K. I. C., Yool, A., Halloran, P. R., and Achterberg, E. P.: On which timescales do gas transfer velocities control North Atlantic CO2 flux variability?, Global Biogeochemical Cycles, 30, 787–802, https://doi.org/10.1002/2015GB005267, https://agupubs.onlinelibrary.wiley.com/doi/abs/10.1002/2015GB005267, 2016.

Desmit, X., Nohe, A., Borges, A. V., Prins, T., Cauwer, K. D., Lagring, R., Zande, D. V. d., and Sabbe, K.: Changes in chlorophyll concentration and phenology in the North Sea in relation to de-eutrophication and sea surface warming, Limnology and Oceanography, 65, 828–847, https://doi.org/10.1002/lno.11351, https://aslopubs.onlinelibrary.wiley.com/doi/abs/10.1002/lno.11351, _eprint: https://aslopubs.onlinelibrary.wiley.com/doi/pdf/10.1002/lno.11351, 2020.

Dickson, A. and Millero, F.: A comparison of the equilibrium constants for the dissociation of carbonic acid in seawater media, Deep-Sea Res. Pt I, 34, 1733 – 1743, https://doi.org/10.1016/0198-0149(87)90021-5, 1987.

Dickson, A. G.: Standard potential of the reaction: AgCl(s) + 12H2(g) = Ag(s) + HCl(aq), and and the standard acidity constant of the ion HSO4 in synthetic sea water from 273.15 to 318.15 K, The Journal of Chemical Thermodynamics, 22, 113–127, https://doi.org/10.1016/0021-9614(90)90074-Z, http://www.sciencedirect.com/science/article/pii/002196149090074Z, 1990.

Fay, A. R. and McKinley, G. A.: Correlations of surface ocean pCO2 to satellite chlorophyll on monthly to interannual timescales, Global Biogeochemical Cycles, 31, 436–455, https://doi.org/10.1002/2016GB005563, https://agupubs.onlinelibrary.wiley.com/doi/abs/10.1002/2016GB005563, 2017.

Fröb, F., Olsen, A., Becker, M., Chafik, L., Johannessen, T., Reverdin, G., and Omar, A.: Wintertime fCO2 Variability in the Subpolar North Atlantic Since 2004, Geophysical Research Letters, 46, 1580–1590, https://doi.org/10.1029/2018GL080554, https://agupubs.onlinelibrary.wiley.com/doi/abs/10.1029/2018GL080554, 2019.

Gregg, W. W., Casey, N. W., and Rousseaux, C. S.: Sensitivity of simulated global ocean carbon flux estimates to forcing by reanalysis products, Ocean Modelling, 80, 24–35, https://doi.org/10.1016/j.ocemod.2014.05.002, http://www.sciencedirect.com/science/article/pii/S1463500314000651, 2014.

Griffiths, J. R., Kadin, M., Nascimento, F. J. A., Tamelander, T., Törnroos, A., Bonaglia, S., Bonsdorff, E., Brüchert, V., Gårdmark, A., Järnström, M., Kotta, J., Lindegren, M., Nordström, M. C., Norkko, A., Olsson, J., Weigel, B., Žydelis, R., Blenckner, T., Niiranen, S., and Winder, M.: The importance of benthic–pelagic coupling for marine ecosystem functioning in a changing world, Global Change Biology, 23, 2179–2196, https://doi.org/10.1111/gcb.13642, https://onlinelibrary.wiley.com/doi/abs/10.1111/gcb.13642, 2017.

Gruber, N., Clement, D., Carter, B. R., Feely, R. A., Heuven, S. v., Hoppema, M., Ishii, M., Key, R. M., Kozyr, A., Lauvset, S. K., Monaco, C. L., Mathis, J. T., Murata, A., Olsen, A., Perez, F. F., Sabine, C. L., Tanhua, T., and Wanninkhof, R.: The oceanic sink for anthropogenic CO2 from 1994 to 2007, Science, 363, 1193–1199, https://doi.org/10.1126/science.aau5153, http://science.sciencemag.org/content/363/6432/1193, 2019.

Ho, D. T. and Wanninkhof, R.: Air–sea gas exchange in the North Atlantic: 3He/SF6 experiment during GasEx-98, Tellus B: Chemical and Physical Meteorology, 68, 30 198, https://doi.org/10.3402/tellusb.v68.30198, https://doi.org/10.3402/tellusb.v68.30198, 2016.

Jones, S. D., Quéré, C. L., Rödenbeck, C., Manning, A. C., and Olsen, A.: A statistical gap-filling method to interpolate global monthly surface ocean carbon dioxide data, Journal of Advances in Modeling Earth Systems, 7, 1554–1575, https://doi.org/10.1002/2014MS000416, https://agupubs.onlinelibrary.wiley.com/doi/abs/10.1002/2014MS000416, 2015.

Kanamitsu, M., Ebisuzaki, W., Woollen, J., Yang, S.-K., Hnilo, J. J., Fiorino, M., and Potter, G. L.: NCEP–DOE AMIP-II Reanalysis (R-2), Bull. Amer. Meteor. Soc., 83, 1631–1644, https://doi.org/10.1175/BAMS-83-11-1631, https://journals.ametsoc.org/doi/abs/10.1175/BAMS-83-11-1631, 2002.

Landschützer, P., Gruber, N., Bakker, D. C. E., Schuster, U., Nakaoka, S., Payne, M. R., Sasse, T. P., and Zeng, J.: A neural network-based estimate of the seasonal to inter-annual variability of the Atlantic Ocean carbon sink, Biogeosciences, 10, 7793–7815, https://doi.org/10.5194/bg-10-7793-2013, 2013.

Landschützer, P., Gruber, N., Bakker, D. C. E., and Schuster, U.: Recent variability of the global ocean carbon sink, Global Biogeochem. Cycles, 28, 927–949, https://doi.org/10.1002/2014GB004853, 2014.

Landschützer, P., Gruber, N., and Bakker, D. C. E.: Decadal variations and trends of the global ocean carbon sink, Global Biogeochemical Cycles, 30, 1396–1417, https://doi.org/10.1002/2015GB005359, https://agupubs.onlinelibrary.wiley.com/doi/abs/10.1002/2015GB005359, 2016.

Landschützer, P., Gruber, N., and Bakker, D. C. E.: An updated observation-based global monthly gridded sea surface pCO2 and air-sea CO2 flux product from 1982 through 2015 and its monthly climatology (NCEI Accession 0160558). Version 2.2., 2017.

Landschützer, P., Gruber, N., Bakker, D. C. E., Stemmler, I., and Six, K. D.: Strengthening seasonal marine CO 2 variations due to increasing atmospheric CO 2, Nature Climate Change, 8, 146, https://doi.org/10.1038/s41558-017-0057-x, https://www.nature.com/articles/s41558-017-0057-x, 2018.

Landschützer, P., Ilyina, T., and Lovenduski, N. S.: Detecting Regional Modes of Variability in Observation-Based Surface Ocean pCO2, Geophysical Research Letters, 0, https://doi.org/10.1029/2018GL081756, https://agupubs.onlinelibrary.wiley.com/doi/abs/10.1029/2018GL081756, 2019.

Laruelle, G. G., Dürr, H. H., Slomp, C. P., and Borges, A. V.: Evaluation of sinks and sources of CO2 in the global coastal ocean using a spatially-explicit typology of estuaries and continental shelves, Geophysical Research Letters, 37, https://doi.org/10.1029/2010GL043691, https://agupubs.onlinelibrary.wiley.com/doi/abs/10.1029/2010GL043691, 2010.

Laruelle, G. G., Dürr, H. H., Lauerwald, R., Hartmann, J., Slomp, C. P., Goossens, N., and Regnier, P. a. G.: Global multi-scale segmentation of continental and coastal waters from the watersheds to the continental margins, Hydrology and Earth System Sciences, 17, 2029–2051, https://doi.org/https://doi.org/10.5194/hess-17-2029-2013, https://www.hydrol-earth-syst-sci.net/17/2029/2013/, 2013.

Laruelle, G. G., Landschützer, P., Gruber, N., Tison, J.-L., Delille, B., and Regnier, P.: Global high-resolution monthly pCO_2 climatology for the coastal ocean derived from neural network interpolation, Biogeosciences, 14, 4545–4561, https://doi.org/https://doi.org/10.5194/bg-14-4545-2017, https://www.biogeosciences.net/14/4545/2017/, 2017.

Laruelle, G. G., Cai, W.-J., Hu, X., Gruber, N., Mackenzie, F. T., and Regnier, P.: Continental shelves as a variable but increasing global sink for atmospheric carbon dioxide, Nature Communications, 9, 454, https://doi.org/10.1038/s41467-017-02738-z, https://www.nature.com/articles/s41467-017-02738-z, 2018.

Lauvset, S. K. and Gruber, N.: Long-term trends in surface ocean pH in the North Atlantic, Marine Chemistry, 162, 71–76, https://doi.org/10.1016/j.marchem.2014.03.009, https://www.sciencedirect.com/science/article/pii/S0304420314000607, 2014.

Lauvset, S. K., Gruber, N., Landschützer, P., Olsen, A., and Tjiputra, J.: Trends and drivers in global surface ocean pH over the past 3 decades, Biogeosciences, 12, 1285–1298, https://doi.org/https://doi.org/10.5194/bg-12-1285-2015, https://www.biogeosciences.net/12/1285/2015/, 2015.

Lima, F. P. and Wethey, D. S.: Three decades of high-resolution coastal sea surface temperatures reveal more than warming, Nat Commun, 3, 1–13, https://doi.org/10.1038/ncomms1713, https://www.nature.com/articles/ncomms1713, 2012.

Lind, S., Ingvaldsen, R. B., and Furevik, T.: Arctic warming hotspot in the northern Barents Sea linked to declining sea-ice import, Nature Clim Change, 8, 634–639, https://doi.org/10.1038/s41558-018-0205-y, https://www.nature.com/articles/s41558-018-0205-y, 2018.

Locarnini, R., Mishonov, A., Baranova, O., Boyer, T., Zweng, M., GarciA, H., Reagan, J., Seidov, D., Weathers, K., Paver, C., and Smoylar, I.: World Ocean Atlas 2018, Volume 1: Temperature, A. Mishonov Technical Ed., 2018.

Loose, B., McGillis, W. R., Schlosser, P., Perovich, D., and Takahashi, T.: Effects of freezing, growth, and ice cover on gas transport processes in laboratory seawater experiments, Geophysical Research Letters, 36, https://doi.org/10.1029/2008GL036318, https://agupubs.onlinelibrary.wiley.com/doi/abs/10.1029/2008GL036318, 2009.

Mehrbach, C., Culberson, C., Hawley, J., and Pytkowicz, R.: Measurement of the apparent dissociation constants of carbonic acid in seawater at atmospheric pressure, Limnol. Oceanogr., 18, 897–907, 1973.

Meyer, M., Pätsch, J., Geyer, B., and Thomas, H.: Revisiting the Estimate of the North Sea Air-Sea Flux of CO2 in 2001/2002: The Dominant Role of Different Wind Data Products, Journal of Geophysical Research: Biogeosciences, 123, 1511–1525, https://doi.org/10.1029/2017JG004281, https://agupubs.onlinelibrary.wiley.com/doi/abs/10.1029/2017JG004281, 2018.

Müller, J. D., Schneider, B., and Rehder, G.: Long-term alkalinity trends in the Baltic Sea and their implications for CO2-induced acidification, Limnology and Oceanography, 61, 1984–2002, https://doi.org/10.1002/lno.10349, https://aslopubs.onlinelibrary.wiley.com/doi/abs/10.1002/lno.10349, 2016.

Naegler, T.: Reconciliation of excess 14C-constrained global CO2 piston velocity estimates, Tellus B: Chemical and Physical Meteorology, 61, 372–384, https://doi.org/10.1111/j.1600-0889.2008.00408.x, https://doi.org/10.1111/j.1600-0889.2008.00408.x, 2009.

Nondal, G., Bellerby, R. G. J., Oldenc, A., Johannessena, T., and Olafssond, J.: Optimal evaluation of the surface ocean CO2 system in the northern North Atlantic using data from voluntary observing ships, Limnol. Oceanogr., 7, 109–118, 2009.

Omar, A. M., Olsen, A., Johannessen, T., Hoppema, M., Thomas, H., and Borges, A. V.: Spatiotemporal variations of f CO2 in the North Sea, Ocean Sci., p. 13, 2010.

Omar, A. M., Thomas, H., Olsen, A., Becker, M., Skjelvan, I., and Reverdin, G.: Trend of ocean acidification and pCO2 in the northern North Sea, 2004-2015, Journal of Geophysical Research - Biogeosciences, 2019.

Oziel, L., Neukermans, G., Ardyna, M., Lancelot, C., Tison, J.-L., Wassmann, P., Sirven, J., Ruiz-Pino, D., and Gascard, J.-C.: Role for Atlantic inflows and sea ice loss on shifting phytoplankton blooms in the Barents Sea, Journal of Geophysical Research: Oceans, pp. 5121–5139, https://doi.org/10.1002/2016JC012582@10.1002/(ISSN)2169-9291.ARCTICJOINT, https://agupubs.onlinelibrary.wiley.com/doi/abs/10.1002/2016JC012582%4010.1002/%28ISSN%292169-9291.ARCTICJOINT, 2016.

Parard, G., Charantonis, A. A., and Rutgersson, A.: Using satellite data to estimate partial pressure of CO_2 in the Baltic Sea: PARTIAL PRESSURE OF CO_2 VARIABILITY, Journal of Geophysical Research: Biogeosciences, 121, 1002–1015, https://doi.org/10.1002/2015JG003064, http://doi.wiley.com/10.1002/2015JG003064, 2016.

Parard, G., Rutgersson, A., Raj Parampil, S., and Charantonis, A. A.: The potential of using remote sensing data to estimate air–sea CO₂ exchange in the Baltic Sea, Earth System Dynamics, 8, 1093–1106, https://doi.org/10.5194/esd-8-1093-2017, https://www.earth-syst-dynam.net/8/1093/2017/, 2017.

Pierrot, D., Neill, C., Sullivan, K., Castle, R., Wanninkhof, R., Lüger, H., Johannessen, T., Olsen, A., Feely, R. A., and Cosca, C. E.: Recommendations for autonomous underway $p\mathrmCO_2$ measuring systems and data-reduction routines, Surface Ocean CO2 Variability and Vulnerabilities, 56, 512–522, https://doi.org/10.1016/j.dsr2.2008.12.005, 2009.

Roobaert, A., Laruelle, G. G., Landschützer, P., and Regnier, P.: Uncertainty in the global oceanic CO_2 uptake induced by wind forcing: quantification and spatial analysis, Biogeosciences, 15, 1701–1720, https://doi.org/https://doi.org/10.5194/bg-15-1701-2018, https://www.biogeosciences.net/15/1701/2018/, 2018.

Rödenbeck, C., Keeling, R. F., Bakker, D. C. E., Metzl, N., Olsen, A., Sabine, C., and Heimann, M.: Global surface-ocean pCO2 and sea–air CO2 flux variability from an observation-driven ocean mixed-layer scheme, Ocean Sci., 9, 193–216, https://doi.org/10.5194/os-9-193-2013, https://www.ocean-sci.net/9/193/2013/, 2013.

Rödenbeck, C., Bakker, D. C. E., Metzl, N., Olsen, A., Sabine, C., Cassar, N., Reum, F., Keeling, R. F., and Heimann, M.: Interannual sea–air CO_2 flux variability from an observation-driven ocean mixed-layer scheme, Biogeosciences, 11, 4599–4613, https://doi.org/https://doi.org/10.5194/bg-11-4599-2014, https://www.biogeosciences.net/11/4599/2014/bg-11-4599-2014.html, 2014.

Rödenbeck, C., Bakker, D. C. E., Gruber, N., Iida, Y., Jacobson, A. R., Jones, S., Landschützer, P., Metzl, N., Nakaoka, S., Olsen, A., Park, G.-H., Peylin, P., Rodgers, K. B., Sasse, T. P., Schuster, U., Shutler, J. D., Valsala, V., Wanninkhof, R., and Zeng, J.: Data-based estimates of the ocean carbon sink variability – first results of the Surface Ocean $p\mathrm{CO_2}$ Mapping intercomparison (SOCOM), Biogeosciences, 12, 7251–7278, https://doi.org/https://doi.org/10.5194/bg-12-7251-2015, https://www.biogeosciences.net/12/7251/2015/, 2015.

Salt, L. A., Thomas, H., Prowe, A. E. F., Borges, A. V., Bozec, Y., and Baar, H. J. W. d.: Variability of North Sea pH and CO2 in response to North Atlantic Oscillation forcing, Journal of Geophysical Research: Biogeosciences, 118, 1584–1592, https://doi.org/10.1002/2013JG002306, https://agupubs.onlinelibrary.wiley.com/doi/abs/10.1002/2013JG002306, 2013.

Schiettecatte, L. S., Thomas, H., Bozec, Y., and Borges, A. V.: High temporal coverage of carbon dioxide measurements in the Southern Bight of the North Sea, Marine Chemistry, 106, 161–173, https://doi.org/10.1016/j.marchem.2007.01.001, http://www.sciencedirect.com/science/article/pii/S0304420307000023, 2007.

Schneider, B. and Müller, J. D.: Biogeochemical Transformations in the Baltic Sea: Observations Through Carbon Dioxide Glasses, Springer Oceanography, Springer International Publishing, https://www.springer.com/gp/book/9783319616988, 2018.

Sharples, J., Ross, O. N., Scott, B. E., Greenstreet, S. P. R., and Fraser, H.: Inter-annual variability in the timing of stratification and the spring bloom in the North-western North Sea, Cont.Shelf Res., 26, 733–751, https://doi.org/10.1016/j.csr.2006.01.011, https://abdn.pure.elsevier.com/en/publications/inter-annual-variability-in-the-timing-of-stratification-and-the-, 2006.

Thomas, H., Bozec, Y., Elkalay, K., and Baar, H. J. W. d.: Enhanced Open Ocean Storage of CO2 from Shelf Sea Pumping, Science, 304, 1005–1008, https://doi.org/10.1126/science.1095491, https://science.sciencemag.org/content/304/5673/1005, 2004.

Thomas, H., Friederike Prowe, A. E., van Heuven, S., Bozec, Y., de Baar, H. J. W., Schiettecatte, L.-S., Suykens, K., Koné, M., Borges, A. V., Lima, I. D., and Doney, S. C.: Rapid decline of the CO2 buffering capacity in the North Sea and implications for the North Atlantic Ocean, Global Biogeochemical Cycles, 21, https://doi.org/10.1029/2006GB002825, https://agupubs.onlinelibrary.wiley.com/doi/full/10.1029/2006GB002825, 2007.

Uppström, L. R.: The boron/chlorinity ratio of deep-sea water from the Pacific Ocean, Deep Sea Research and Oceanographic Abstracts, 21, 161–162, https://doi.org/10.1016/0011-7471(74)90074-6, http://www.sciencedirect.com/science/article/pii/0011747174900746, 1974.

van Heuven, S., Pierrot, D., Lewis, E., and Wallace, D.: {MATLAB} Program Developed for {CO}$_2$ System Calculations. {ORNL/CDIAC}-105b., 2009.

Wanninkhof, R.: Relationship between wind speed and gas exchange over the ocean revisited: Gas exchange and wind speed over the ocean, Limnology and Oceanography: Methods, 12, 351–362, https://doi.org/10.4319/lom.2014.12.351, http://doi.wiley.com/10.4319/lom.2014.12.351, 2014.

Weiss, R. F.: Carbon dioxide in water and seawater: The solubility of a non-ideal gas, Mar. Chem., 2, 203–215, 1974.

Wesslander, K., Omstedt, A., and Schneider, B.: Inter-annual and seasonal variations in the air–sea CO2 balance in the central Baltic Sea and the Kattegat, Continental Shelf Research, 30, 1511–1521, http://www.academia.edu/16389763/Inter-annual_and_seasonal_variations_in_the_air_sea_CO2_balance_in_the_central_Baltic_Sea_and_the_Kattegat, 2010.

Wollast, R.: Evaluation and comparison of the global carbon cycle in the coastal zone and in the open ocean, in: The Sea, edited by Brink, K. H. and Robinson, A. R., pp. 213–252, John Wiley & Sons, New York, 1998.

Yasunaka, S., Siswanto, E., Olsen, A., Hoppema, M., Watanabe, E., Fransson, A., Chierici, M., Murata, A., Lauvset, S. K., Wanninkhof, R., Takahashi, T., Kosugi, N., Omar, A. M., Heuven, S. v., and Mathis, J. T.: Arctic Ocean CO_2 uptake: an improved multiyear estimate of the air–sea CO_2 flux incorporating chlorophyll *a* concentrations, Biogeosciences, 15, 1643–1661, https://doi.org/https://doi.org/10.5194/bg-15-1643-2018, https://www.biogeosciences.net/15/1643/2018/, 2018.